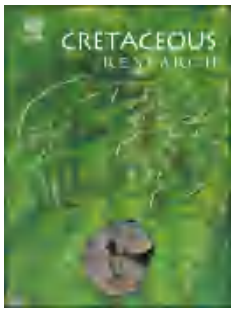

New brevirostrines (Crocodylia, Brevirostres) from the Upper Cretaceous of China

Xiao-Chun Wu, Yan-Chao Wang, Hai-Lu You, Yu-Qing Zhang, Lai-Ping Yi

PII: S0195-6671(22)00314-7

DOI: https://doi.org/10.1016/j.cretres.2022.105450

Reference: YCRES 105450

To appear in: *Cretaceous Research*

Received Date: 31 May 2022

Revised Date: 5 December 2022

Accepted Date: 8 December 2022

Please cite this article as: Wu, X.-C., Wang, Y.-C., You, H.-L., Zhang, Y.-Q., Yi, L.-P., New brevirostrines (Crocodylia, Brevirostres) from the Upper Cretaceous of China, *Cretaceous Research*, https://doi.org/10.1016/j.cretres.2022.105450.

Author Statement

All authors have contributed equally to the conception, writing, and revision of this manuscript.

New brevirostrines (Crocodylia, Brevirostres) from the Upper Cretaceous of China

Xiao-Chun Wu[1*], Yan-Chao Wang[2,3,4], Hai-Lu You[2,3,4*], Yu-Qing Zhang[5,6], and Lai-Ping Yi[7]

[1]*Canadian Museum of Nature, PO Box 3443 STN "D", Ottawa, ON KIP 6P4, Canada* xcwu@nature.ca

[2]*Key Laboratory of Vertebrate Evolution and Human Origins, Institute of Vertebrate Paleontology and Paleoanthropology, Chinese Academy of Sciences, Beijing, 100044, P.R. China* wangyanchao@ivpp.ac.cn, *youhailu@ivpp.ac.cn*

[3]*CAS Center for Excellence in Life and Paleoenvironment, Beijing, 100044, P.R. China*

[4]*College of Earth and Planetary Sciences, University of Chinese Academy of Sciences, Beijing, P.R. China*

[5]*No. 208 Hydrogeological and Engineering Geological Team, Chongqing Bureau of Geological and Mineral Resource Exploration and Development, Chongqing, P.R. China* 2788827552@qq.com

[6]*Chongqing Key Laboratory of Paleontology and Paleoenvironment Co-evolution (Sichuan-Chongqing Joint Construction), Chongqing, P.R. China*

[7]*Ganzhou Museum, Ganzhou City, Ganzhou Administrative Distract, Jiangxi province, P.R. China* 476470435@qq.com

Abstract: A new alligatoroid, *Eurycephalosuchus gannanensis* gen. et sp. nov. and an undetermined brevirostrine, Brevirostres gen. et sp. indet. are described. They are preserved

together in the Upper Cretaceous of Jiangxi Province, China. *Eurycephalosuchus gannanensis* is established based on a well-preserved skull with the mandible and some postcranial elements, and Brevirostres gen. et sp. indet. is represented by the right scapula and coracoid. *Eurycephalosuchus gannanensis* is assigned to Alligatoroidea and phylogenetically nested within a sub-group of Orientalosuchina with other four genera from China and Vietnam. *Eurycephalosuchus gannanensis* differs from all other orientalosuchines primarily in the short and broad appearance of its skull, the abnormally short (anteroposteriorly narrow) skull table, the exclusion of the parietal from the occipital ridge posteriorly, the postdentary part of the mandible much deeper than the anterior part dorsoventrally, the splenial excluded from the mandibular symphysis, and the external mandibular fenestra small and nearly vertical in orientation. It is different from Brevirostres gen. et sp. indet. in that the distal end of the scapular blade is relatively broader, and the anterior margin of the coracoid is more concave in addition to the smaller size. The discovery of the two new forms not only enriches the diversity of the local fauna but also confirms the monophyly of Orientalosuchina and the Asian dispersal event of the clade after diverging from the mainline rather than a sub-lineage of Alligatoroidea in the Late Cretaceous.

Keywords: Brevirostres; Alligatoroidea; Orientalosuchina; Upper Cretaceous; China

1. Introduction

In recent years, there has been several fossil reptiles discovered in the Upper Cretaceous red beds in Municipality of Ganzhou City (MGC), the southern part (Gannan) of Jiangxi Province. Most of those fossils were exposed by the construction activities associated with local infrastructure development in some districts of MGC. Up to the present, the reptile fossils excavated include a few dinosaur species (Xu and Han, 2010; Wang et al., 2013; Wei et al., 2013; Lü et al., 2013a, 2013b, 2014, 2015, 2016, 2017; Xing et al., 2020a), two lizards (Mo et al., 2010, 2012), two turtles (Tong and Mo, 2010), and dinosaur eggs including those with embryos (Sato et al., 2005; Cheng et al., 2008; Xing et al., 2020b, 2021). In addition to the vertebrate fossils mentioned above, there is a crocodylian reptile, *Jiangxisuchus nankangensis* described by Li et al. in 2019, which was soon assigned to Orientalosuchina by Massonne et al. (2019). Shan et al. (2021) recognized another orientalosuchine from China and further confirmed the orientalosuchine status of *Jiangxisuchus nankangensis*. Up to the present, there have been six orientalosuchines known from southeastern Asia and southeast China, including the type species *Orientalosuchus naduongensis* from Vietnam (Massonne et al., 2019), *Krabisuchus siamogallicus* from Thailand (Martin and Lauprasert, 2010), and four Chinese species: *Eoalligator chunyii* (Young, 1964), *Protoalligator huiningensis* (Wang et al., 2016 = *Eoalligator huiningensis* Young, 1982), *Jiangxisuchus nankangensis*, and *Dongnanosuchus hsui* (Shan et al., 2021).

In 2021, a new crocodylian specimen was excavated in a block of matrix from the Upper Cretaceous of MGC. The fossil locality situates at Shahe Town of Zhanggong District of MGC, about 2 km northeast to the Ganzhou Railway Station or about 50 km northeast to the quarry of *Jiangxisuchus nankangensis* in Nankang District of MGC (Fig. 1). The new crocodylian specimen represents the seventh orientalosuchine known from Asia. Along with the articulated

section of the postcranial skeleton of the new crocodylian, there is a big and articulated pair of the right scapula and coracoid. This big pair evidently belongs to another species in terms of morphological differences in addition to their large size, although its taxonomy cannot be determined within Brevirostres based on the current material. Here we mainly describe the new orientalosuchine, focusing on its osteological anatomy, taxonomy, and phylogeny. The new discovery not only illustrates the diversity of the local crocodylians but also provides a chance to test the hypotheses made by previous studies on the early history of alligatoroid crocodylians, particularly the internal and external relationships of Orientalosuchina.

2. Geological setting

The new crocodylian specimens were recovered from the redbeds in the construction site of Qingfeng Pharmaceutical Manufactory (QPM) at the Industrial Park of Shahe Town (IPST), Zhanggong subdistrict of MGC. The redbeds of the site of QPM belong to the Upper Cretaceous Hekou Formation (He et al., 2017). The formation of IPST yields not only the new crocodylians but also dinosaurs, turtles and dinosaur eggs including the elongatoolithid egg with an embryo (He et al., 2017; Xing et al., 2021). The Upper Cretaceous redbeds of MGC are generally assigned to the Ganzhou Group or the Guifeng Group in ascending order, the former group is further divided into the Maodian and Zhoutian formations while the latter comprises the Hekou and Tangbian formations (the Upper Cretaceous) as well as the Lianhe Formation (the uppermost Cretaceous-Paleogene) (see Wen et al., 2016). On the other hand, the redbeds of MGC are traditionally correlated to the Upper Cretaceous Nanxiong Group/Formation (Jiangxi Bureau of Geology and Mineral Resources, 1984), although this

correlation is inconsistent with other studies (see citations of Xing et al., 2021). A related paleomagnetic study on the Ganzhou redbeds suggests that the age of the Guifeng Group ranges from 71.4 to 65.0 Ma (Zuo et al., 1999). In this case, the bottom position of the Hekou Formation within the Guifeng Group indicates that the formation should be the early Maastrichtian in age. As indicated by the geological map of the Upper Cretaceous in MGC (He et al., 2017), the outcrops of the Hekou Formation distribute extensively, covering the vast area of Nankang District, including the Nankang city centre near which *Jiangxisuchus nankangensis* was collected, although the redbeds yielding the orientalosuchine, other vertebrate fossils, and dinosaur eggs were originally correlated by Li et al. (2019) and other studies to the strata of the Upper Cretaceous (Maastrichtian) of the Nanxiong Formation or group (Xu and Han, 2010; Wang et al., 2013; Lü et al., 2014, 2015, 2016).

3. Material and methods

The crocodylian specimens studied here are housed in the Collections of Institute of Vertebrate Paleontology and Paleoanthropology, Chinese Academy of Sciences, Beijing, China. It comprises the skull with the mandible occluded and some postcranial elements. We prepared the crocodylian specimens using mechanical tools (pneumatic chisels) and photographed them from various perspectives with a Nikon D610 digital camera. The figures were prepared using Adobe Photoshop 2020 and Illustrator 2020. We made line drawings based on the reference photographs and checked them against the original specimens. Measurements of selected skull regions were taken directly from the original specimens. The phylogenetic analyses were performed using TNT v.1.5 (Goloboff and Catalano, 2016).

Institutional abbreviations. IVPP, Institute of Vertebrate Paleontology and Paleoanthropology, Chinese Academy of Sciences, Beijing, China; IRSNB, Institut Royal des Sciences Naturelles de Belgique, Brussels, Belgium.

Anatomical abbreviations. acr, acromial crest; amc, adductor muscle chamber; an, angular; ana, atlantal neural arch; ar, articular; arf, articular fossa; avs, anteroventral process of surangular; ax, axis; axns, axial neural spine; bco, big coracoid; bo, basioccipital; bs, basisphenoid; bsc, big scapula; cev, centrum of a vertebra; ch, internal choana; cgl, coracoid glenoid fossa; co, coracoid; cof, coracoid foramen; cr, cervical rib; cp, capitulum; ctmp, concavity for attachment of tendon for adductor mandibulae posterior; d, dentary; dpc, deltopectoral crest; dip, diapophysis; dth, dentary tooth; dr, dorsal rib; dvt, dorsal vertebrae; ec, ectopterygoid; ecq, exit for cranio-quadrate canal; emf, external mandibular fenestra; en, external naris; eo, exoccipital; f, frontal; faë, foramen aërum; fan, facet for angular; fatc, facet for the atlantal centrum; fca, foramen for carotid artery; fcq, foramen for cranio-quadrate canal; fdsa, foramen between dentary and surangular; fio, foramen for intermandibularis oralis; fm, foramen magnum; fsc, facet for scapula; fr2, facet for the 2nd rib; gl, glenoid fossa; gev, groove for ear flap; hp, hypophyseal process; hy, hyoid; ic, foramen for internal carotid artery; inc, interclavicle; itf, infratemporal fenestra; j, jugal; l, lacrimal; let, lateral exis of Eustachian tube; los, lateral osteoderm; lt, lateral tubercle; m, maxilla; mdq, medial condyle of quadrate; mec, middle ear chamber; men, margin of external naris; met, median exit of Eustachian tube; mif, margins of incisive foramen; ms, mandibular symphysis; mt, medial tubercule; mth, maxillary tooth; n, nasal; nca, neural canal; nsp, neural spine; ob, orbit; oc, occipital condyle; os, osteoderm; otp. odontoid process; p, parietal; pap, parapophysis; pf, prefrontal; pl, palatine; pm, premaxilla; pmth, premaxillary teeth; po, postorbital; pop, paroccipital process; poz,

postzygapophysis;; prz,, prezygapophysis; pt, pterygoid; ptf, remnant of posttemporal fenestra; q, quadrate; qj, quadratojugal; rap, retroarticular process; rhc, radial hemicondyle; sa, surangular; sc, scapula; sch, septum of internal choana; sgl, scapular glenoid fossa; so, supraoccipital; sof, suborbital fenestra; sp, splenial; sq, squamosal; sqj, quadratojugal spine; stf, supratemporal fossa; vos, ventral osteoderm; tb, tuberculum; trf, transverse flange; vt, vertebra; uhc, ulnar hemicondyle; IX-XII, foramina for the 9^{th} to 12^{th} cranial nerves.

4. Systematic paleontology

EUSUCHIA Huxley, 1875

CROCODYLIA Gmelin, 1789 (sensu Clark in Benton and Clark, 1988)

BREVIROSTRES von Zittel, 1890 (sensu Brochu, 2003)

ALLIGATOROIDEA Gray, 1844, (sensu Brochu, 2003)

GLOBIDONTA Brochu, 1999

ORIENTALOSUCHINA Massonne et al., 2019

Genus *Eurycephalosuchus* gen. nov.

Etymology. From Greek *eurys*, wide/broad, Greek *kephale*, head, and Greek *Sobek*, the Egyptian crocodile god, in reference to the short and broad skull of this crocodylian.

Diagnosis. A small to medium-sized alligatoroid, differing from other taxa in the unique combination of following derived characters: Skull short and broad, nearly equal in width and length (apomorphic); skull table remarkedly short, less than half transverse width in length

(apomorphic); supraoccipital broadly exposed on skull roof; parietal excluded by supraoccipital-squamosal contact from posterior (occipital) margin of skull table; exoccipitals broadly contact each other dorsal to foramen magnum; dermal bones of skull roof overhang rims of supratemporal fenestra; dorsoventral depth of mandible across centre of external mandibular fenestra more than three times minimal depth of dentary behind the fourth caniniform tooth; splenial excluded from mandibular symphysis, external mandibular fenestra small and nearly vertical in orientation, neural spine of the 15th vertebra becoming much broader than that of the 14th and more anterior vertebrae, and both sides of scapular blade flaring dorsally.

Type species: *Eurycephalosuchus gannanensis* sp. nov.

(urn: lsid:zoobank.org:pub:F885DE95-18D9-4F3D-86A7-3589E9CF7BEE)

Figs. 2–12

Holotype. IVPP V 31110. The specimen includes the skull with the mandible occluded, 14 post-axial vertebrae, about 15 ribs, left scapula and coracoid, left humerus, and some osteoderms.

Locality and horizon. The construction site of QPM at IPST, Zhanggong District of MGC, Jiangxi Province, China; Hekou Formation, Upper Cretaceous (Maastrichtian) (Zuo et al., 1999).

Etymology. Referring to Chinese Gannan, southern part of Jiangxi Province, where the specimen was collected, plus -*ensis*, traditional suffix for specific nomina of the animal that is named after the place where the animal was first found.

Diagnosis. As for the genus.

Description

General features: The skull and mandible are heavily built. The skull is nearly complete and tightly occluded with the mandible (Figs. 2-4; Fig. S1A in the online supplementary data). It was compressed forwards, especially on its right side, so that the frontal and two prefrontals now slightly overlap the posterior edges of two nasals and the anteromedial margin of the right lacrimal. In addition, the frontal overlaps the anterior portion of the left postorbital posteriorly. This forward deformation caused the size of the orbits to have shrunk smaller and the quadrate to have moved anteriorly, being detached from the quadratojugal laterally and the jaw joint posteriorly on the right side (Fig. 5). The forward deformation also caused the anterior edge of the orbit to tilt deeply forward, forming an angle greater than 45 degrees between the anterior and ventral margins of the orbit in lateral view (Fig. 3A, B). The skull is short but broad and its left side is less affected by the forward deformation. The skull is 14.31 mm in length (from the anterior tip of the snout to the posterior margin of the skull table), which should be added with 5 mm assumably shortened by the forward deformation of the skull as suggested by the length reduction of the orbits, especially the right one which was obviously shortened by the lacrimal moving backwards into it. In this case, the skull length may have reached 14.81 cm in life, being about same to its maximal width across the quadratojugals (14.81 cm). The skull may have reached 16.37 cm in life if it is measured from the anterior tip of the snout to the posterior end of the quadrate condyle and then the skull is slightly longer than wide. Such a broadened skull is unique within Orientalosuchina. The snout is correlatedly short, being only 9.63 cm long, even shorter than its the base width of 10.12 cm (across the anterior margins of the orbits), which is also unusual within Orientalosuchina or even Alligatoroidea. The skull table is shorter than wide

as in other crocodylians, but it is here unbelievably short, with its length less than one third of its width (3.55/8.55 cm), which is again peculiar within Orientalosuchina or even Alligatoroidea.

The length of the right ramus of the mandible was little affected by the forward deformation of the skull and this ramus is 18.3 cm long, about 1.15 cm longer than the left ramus (17.15 cm). The anterior portion of the mandible is very shallow, and the postdentary part of the mandible is extremely deep, i.e., the minimal depth of the mandible posterior to the fourth dentary tooth is less than 15 mm but the maximal depth across the centre of the external mandibular fenestra reaches 49.5 mm, more than three times the minimal depth; this difference is much stronger than that seen in *Orientalosuchus naduongensis* Massonne et al., 2019. External ornamentation of the skull and mandibular elements consists of pits and coarse ridges.

Openings: It is uncertain whether the external naris is separate or confluent due to the damage of the anterior end of the opening (Fig. 3A, B; Fig. S1A in the online supplementary data). It is much wider than long if it is single as in *Orientalosuchus naduongensis* (see Table 1). Both orbits, especially the right, are distorted by the forward deformation of the skull, although they are obviously much larger than the supratemporal fossa. The dorsal margin of the orbit does not rise to form a rim as in *Jiangxisuchus nankangensis*. The left supratemporal fossa is little distorted, having a roughly triangular outline with a sharp angle pointing forward. It is wider than long. All bones surrounding this fossa, except for the frontal, overhangs the margins of the fossa, which contrasts the situation of other orientalosuchines where the relevant part is preserved. In addition to the orbits, the infratemporal fenestrae are also heavily distorted among skull openings. The ventral margin of the left infratemporal fenestra is nearly complete, which is longer than the supratemporal fenestra. The choanae are divided by a lamina-like septum into two as in other orientalosuchines where the relevant part is preserved, and the right half is

231 distorted toward the left side (Fig. 4A, B; Fig. SB in the online supplementary data). Both
232 suborbital fenestrae are slightly distorted, bending downwards due to the forward deformation of
233 the skull. It is large and nearly as long as the palatine. The left is better preserved than the right;
234 it is much longer than wide (see Table 1). The fenestra is roughly triangular in outline and
235 anterolaterally-posteromedially oriented. The medial margin is nearly straight. The left external
236 mandibular fenestra of the mandible is nearly complete and irregularly rectangular in outline. It
237 is anteroventrally-posterodorsally oriented (Fig. 3A, B). This fenestra is dorsally narrow, being
238 dorsoventrally much deeper than anteroposteriorly wide.

239 *Skull elements*: Both premaxillae are nearly complete except for the anterior margin of
240 the external naris. It is longer than wide in dorsal view, with a constriction caused by a notch
241 present at the lateral end of the premaxillary–maxillary suture (Figs. 2A, B; 3A, B). The notch is
242 moderately deep in both dorsal and ventral views as well as in lateral view as in some of other
243 crocodylians such as *Orientalosuchus naduongensis*, *Leidyosuchus* (Wu et al., 2001) but not
244 *Jiangxisuchus nankangensis* or *Dongnanosuchus hsui* where the notch is dorsally and ventrally
245 shallow. The two premaxillae are separated by two nasals posterior to the external naris along the
246 midline as in *Orientalosuchus naduongensis*, *Jiangxisuchus nankangensis*, and *Dongnanosuchus*
247 *hsui*. The dorsal surface of the premaxilla is not elevated along the lateral margin of the naris.
248 The maxillary process of the bone is short, being not exceeding the posterior margin of the third
249 maxillary tooth, this contrasts to that in *Jiangxisuchus nankangensis*, *Dongnanosuchus hsui*, and
250 *Orientalosuchus naduongensis*. Ventrally, the premaxillae are extensively concealed by the
251 occlusion of the mandible. The incisive foramen is minimally exposed in the external naris (Fig.
252 2A, B). It is wider than long (see table 1) as in *Orientalosuchus naduongensis* although its
253 anterior margin is slightly damaged in the former.

The strap-like nasals have a pointed anterior process. Their posterior ends are covered by the displacement of the frontals and prefrontals due to the forward deformation of the skull, but it shows a tendency to narrow posteriorly (Fig. 2A, B). The anterior process of each nasal meets its counterpart along the midline and enters the external naris as in *Jiangxisuchus nankangensis* or *Dongnanosuchus hsui* or *Orientalosuchus naduongensis*, but it is narrower than that of the latter three. The nasals widen slightly in the posterior direction as they approach the lacrimals. It is uncertain whether they, from the point of contact, taper off to a wedge-shaped process that does not directly abut its counterpart. Sutures of the nasal with the premaxilla, maxilla, lacrimal, and prefrontal form a convex line towards the lateral side as in *Krabisuchus siamogallicus* and the aforementioned three orientalosuchines. The sutural contact of the nasal with the frontal is covered by the frontal due to the forward deformation of the skull.

The maxilla is the broadest bone on the dorsal surface of the skull among the skull elements, being broader in dorsal view and much longer in lateral view than the two nasals (Figs. 2A, B; 3A, B). It narrows anteriorly into a wedge-shaped process, slightly constricts posterior to the fifth maxillary tooth, and then slightly broadens in dorsal view. Posteriorly, the maxilla sharply reduces into a process in lateral view. The maxilla possesses a small posterodorsal process inserting between the nasal and lacrimal and terminates posterolaterally along a broadly inclined suture with the jugal. Sutural contacts of the maxilla with the premaxilla, nasal, lacrimal, and jugal are clear on the right side. The maxilla exhibits no significant elevations or depressions on the dorsal surface except for two bulges just dorsal and lateral to the large fifth tooth. In lateral view, the dental margin is strongly concavo-convex as in other orientalosuchines, such as *Dongnanosuchus hsui*, forming two waves (festoons). The peak of the first wave is at the fifth maxillary alveolus and that of the second wave is at the twelfth maxillary alveolus, which is at

277 the eleventh maxillary tooth in *Dongnanosuchus hsui* and *Jiangxisuchus nankangensis*. There are
278 numerous small nutrient foramina dorsal to the tooth row. A fossa medial to the dentition
279 between the seventh and eighth maxillary alveoli is assumably present, which, as shown on the
280 right side, receives a dentary tooth when the jaws are closed. In palatal view, the maxillary-
281 palatine suture is convex toward the maxilla. The maxillary-ectopterygoid suture is concealed by
282 the jaw occlusion. The maxilla terminates anterior to the postorbital bar.

283 The right lacrimal is better preserved. It is much larger than the prefrontal, showing an
284 irregular outline in dorsal view (Fig. 2A, B). It is posteriorly broad and anteriorly narrow. Its
285 anterior margin is sharply convex, wedging into the maxilla and extending forward to
286 approximately the level of the seventh maxillary alveolus as in *Jiangxisuchus nankangensis*.
287 Posteriorly, it forms a narrow posterolateral process with which the lacrimal forms much of the
288 anterior and anteroventral borders of the orbit. Medially, the right lacrimal is overlapped by the
289 prefrontal, but the left lacrimal shows a strongly convex sutural contact with the nasal and
290 prefrontal.

291 The left prefrontal is better preserved than the right one. It is roughly triangular in dorsal
292 view (Fig. 2A, B). Its sutural contact with the lacrimal is nearly straight. Its sutures with frontal
293 and nasal are obscured due to the anterior displacement of the frontal. Posteriorly, the prefrontal
294 forms the anteromedial margin of the orbit.

295 The unpaired frontal is broken into four pieces so that its pointed anterior process is
296 displaced towards left side and its posterolateral portion slightly overlaps the anterior portion of
297 the left postorbital and the main body of the frontal on the right side (Fig. 2A, B). As in other
298 orientalosuchines where it is known, the frontal broadens posteriorly and makes a modest entry
299 into the supratemporal fossa posterolaterally. The dorsal surface of the frontal is gently concave.

The frontal-parietal suture is concavo-convex towards the parietal (Fig. 2C, D). As displayed by the right side, the frontal contributes a small portion to the dorsal margin of the orbit. The interorbital septum is moderately broad, slightly broader than the interfenestral septum of the parietal as in *Dongnanosuchus hsui*. The frontal-postorbital suture, as shown on the right side, is slightly oblique and gently concavo-convex.

The right postorbital is nearly complete, comprising a dorsal body that is roughly rectangular and bears a pointed anteromedial process and a slender descending process forming the dorsal half of the postorbital bar (Figs. 2A, B; 3A, B). The dorsal surface of the body is flat and forms the rounded anterolateral corner of the skull table. It borders the posterodorsal margin of the orbit anteriorly and the anterolateral margin of the supratemporal fossa posteriorly. Posteromedially, the postorbital contributes a small portion to the supratemporal fossa in which it meets the anterolateral corner of the parietal as in *Jiangxisuchus nankangensis* and *Dongnanosuchus shui*. The descending process is broken into two pieces on both sides; it appears to be columnar dorsally and inset medially from the skull table. It flattens ventrally and passes lateral to the ascending process of the jugal (Fig. 3C, D). It is uncertain whether the postorbital contacts the quadrate on the ventral surface of the skull table as in some orientalosuchines such as *Dongnanosuchus hsui*.

The single parietal is laterally concave in the skull roof and forms the medial floor of the supratemporal fossa (Fig. 2). It does not rise to form an elevated rim around but overhangs the medial margin of the fossa. The interfenestral bar is slightly narrower than the interorbital bar as in *Dongnanosuchus hsui*. The parietal contacts the quadrate broadly within the supratemporal fossa but is excluded by the quadrate from the squamosal in the fossa as in *Jiangxisuchus nankangensis* and *Dongnanosuchus hsui* (Fig. 2C, D). The parietal contacts the squamosal

posterolaterally and the supraoccipital posteriorly. The parietal-squamosal suture is nearly straight and the parietal-supraoccipital suture exposed on the skull roof. The dorsal surface of the parietal is gently concave.

The right jugal is nearly complete, being typically triradiate in dorsolateral view (Fig. 2A, B). Its anterior ramus is much broader than, but slightly shorter than the posterior ramus. The former is similar to the latter in length in *Dongnanosuchus shui*. It slightly narrows and inserts between the maxilla and lacrimal anteriorly. The jugal widens posteriorly, reaching its maximum dorsoventral width at the lateral orbital margin, at which point the anterior ramus becomes narrower until it reaches the end. The jugal extends to the quadratojugal anterior to the posteroventral corner of the infratemporal fenestra dorsolaterally while it reaches the quadratojugal anterior to the mandibular condyle ventrolaterally. The jugal forms the posteroventral margin of the orbit and the anterior two-thirds of the ventral margin of the infratemporal fenestra in dorsal view. The infratemporal bar is broad and lateromedially thin. The cylindrical ascending process of the jugal is inset from the surface of the bone and extends dorsally. The process is disarticulated with the descending process of the postorbital dorsally on both sides and it should have formed the lower portion of the postorbital bar in life.

The right quadratojugal is nearly complete except for the anterodorsal end (Fig. 3E, F). It bears a short spine with its distal tip missing. The spine is high in position and is situated between the posterior and superior angles of the infratemporal fenestra. In orientation, the spine is nearly parallel to the posterior margin of the fenestra as in some alligatoroids, such as *Brachychampsa montana* (Brochu, 1999: fig. 25D). The presence of the quadratojugal spine is not reported in other orientalosuchines. The anterior (jugal) process is short and joins the formation of the posterior quarter of the infratemporal bar in dorsal view (Fig. 2A B). In other

orientalosuchines where the relevant part is complete, this process is absent in dorsa view, and the ventral margin of the infratemporal fenestra is entirely formed by the jugal. In lateral view, the anteroventral portion is ornamented by pits and extends posteriorly nearly to the lateral condyle of the quadrate, while the posterodorsal portion is unornamented and narrows dorsally, forming the posterior margin of the infratemporal fenestra. The incompleteness of the posterodorsal extremity leads to an uncertainty if the quadratojugal meets the postorbital or not along the dorsal border of the infratemporal fenestra in life. The quadratojugal-quadrate suture is nearly straight, running anterodorso-posteroventrally as in other orientalosuchines.

The triradiate squamosal forms the posterolateral margin of the supratemporal fossa in dorsal view (Fig. 2). It contacts the postorbital anteriorly, passing below the latter and ending posterodorsal to the base of the postorbital bar as in other orientalosuchines where the relevant part is complete. The squamosal does not enter the dorsal margin of the infratemporal fenestra as in *Dongnanosuchus shui* (Fig. 3C, D). The squamosal extends laterally over the otic aperture to form a deep otic recess and forms the dorsal roof and posterior wall of the aperture itself. In lateral view, the squamosal exhibits a groove for the external ear valve musculature, which traverses the squamosal from its posterior region to the postorbital. The dorsal margin of the groove is straight anteroposteriorly, and the ventral margin of the groove is convex, which differs from that in *Jiangxisuchus nankangensis*, *Dongnanosuchus hsui*, and *Orientalosuchus naduongensis* where the dorsal and ventral margins are parallel. The dorsal one appears inflated and overhangs the ventral one as in the above three orientalosuchines. The squamosal contacts the parietal behind the supratemporal fossa. Its posterolateral process is well developed, and its dorsal surface is nearly flat. The process extends posterolaterally and terminates as a vertically

oriented and unornamented lamina-like structure against the paraoccipital process of the exoccipital posterolaterally and the dorsal surface of the quadrate body ventrally.

Both quadrates are complete (Figs. 2-5). The are complex bones, forming the anterior and ventral margins of the otic recesses. As in other crocodylians or other orientalosuchines, the dorsal and posterior margins of the recess are formed by the squamosal; the quadrate-squamosal suture extends anterodorsally to the posterolateral corner of the recess (Fig. 3C, D). The dorsal surface of the quadrate body is not ornamented and the dorsal prominence, with the squamosal anteriorly and paraoccipital process posteriorly, encloses the cranio-quadrate foramen medially (Fig. 5A, C). The position of the foramen aëreum is close to the medial margin of the bone as in *Jiangxisuchus nankangensis*, *Dongnanosuchus hsui*, and *Orientalosuchus naduongensis*. The lateral condyle is slightly larger than the medial condyle. In dorsal view, the anterodorsal process of the quadrate narrowly enters the orbito-temporal foramen within the supratemporal fossa, which excludes the squamosal from contacting the parietal in the fossa as in *Jiangxisuchus nankangensis*, *Dongnanosuchus hsui*, and *Orientalosuchus naduongensis* (Fig. 2C, D). Ventrally, the quadrate is concave and crests A and B of Iordansky (1973) for the attachments of adductor muscles are well developed. The quadrate extends mediodorsally to meet the pterygoid and, together, underlies the basisphenoid medially.

Palate: The paired palatines are relatively small and slightly shortened by the forward deformation of the skull (Fig. 4A, B). The suborbital fenestra is large, and its long axis is even slightly longer than the palatine as it is in *Jiangxisuchus nankangensis*, *Dongnanosuchus hsui*, and *Orientalosuchus naduongensis*. The palatines make the medial margin of the suborbital fenestrae except for the anteromedial and posteromedial portions. The bone is posteriorly narrow and widens toward its anterior end. It then narrows anteromedially. Its suture with maxilla is

391 nearly straight and runs anteromedially. Its suture with the pterygoid is located anterior to the
392 posterior-most level of the suborbital fenestra as in *Dongnanosuchus hsui*, and *Orientalosuchus*
393 *naduongensis*.

394 The pterygoid is large and broad. Fig. 4A, B). Its suture with the counterpart anterior to
395 the internal choana is obscured by fractures. In ventral view, its anterior portion is relatively
396 narrower than its posterior portion. The flange is massive and extends posteriorly to form a
397 pronounced posterolateral process (Fig. S1B in the online supplementary data), the latter slightly
398 bends anteriorly now due to the forward compression of the skull and should have projected to a
399 level eventually posterior to the posteromedial processes as in other orientalosuchines, such as
400 *Dongnanosuchus hsui*. The posteromedial process is small but well marked, overhanging the
401 braincase in ventral view. The internal choanae are located at the posterior half of the pterygoid
402 and divided by a thin septum that is inset from the surface on which the choanae open to join the
403 pharyngeal cavity. The surface lateral to the choanae is depressed and no evident crest surrounds
404 the choanae as in *Jiangxisuchus nankangensis* and *Dongnanosuchus hsui*. Posterodorsally, the
405 pterygoid underlies the basisphenoid and meets the quadrate. Anteroventrally, the divided
406 pterygoids contribute to the medial part of the posterior margin of the suborbital fenestra and
407 send a short process to join the formation of the septum between the suborbital fenestrae as in
408 *Dongnanosuchus hsui* and *Orientalosuchus naduongensis*. In posterodorsal view, the transverse
409 flange is very concave (Fig. S2A, B in the online supplementary data).

410 Both ectopterygoids are not visible in dorsal view but their pterygoid processes are
411 completely in ventral view (Fig. 4A, B). The pterygoid process tapers off distally and extends
412 posteroventrally along the lateral margin of the pterygoid flange, but it does not reach the caudal
413 end of the flange, about 8 mm apart from the end. The waisted portion between the maxillary and

pterygoid processes is broader than the narrowest part of each palatine, but not as broad as in *Dongnanosuchus hsui* in which it is broader than the narrowest parts of two palatines (Shan et al., 2021: fig. 3.3, 3.4). Anteromedially, the ectopterygoid forms the posterolateral margin of the suborbital fenestra. Anterolaterally, the maxillary process forms the posterolateral margin of the suborbital fenestra, and its relationship with the maxillary alveolar groove is unknown due to the jaw occlusion. Posterolaterally, the jugal process of the left ectopterygoid is complete, it is short and reaches to the base of the descending ramus of the jugal (Fig. S2A, B in the online supplementary data).

Braincase: The supraoccipital is large and broadly exposed on the skull roof so that the parietal is excluded by the supraoccipital from the occipital edge of the skull roof as in *Orientalosuchus naduongensis* (Figs. 2A, B; 5A, B). The supraoccipital-parietal suture is convex, protruding forward into the parietal. The supraoccipital appears irregularly pentagonal in occipital view. It bears a pronounced median ridge, running ventrally along the most part of the bone. The dorsal edge of the bone is convex and joins the formation of the thickened posterior edge of the skull roof, which overhangs the occiput. Ventrally, the supraoccipital does not enter the foramen magnum, about 9 mm apart from the latter. Sutures of the bone with the parietal, squamosal, and exoccipital are clearly marked. There is a small fossa/depression where these bones meet, which may have indicated the place where the posttemporal fenestra was present before the skull reached the adulthood.

The large exoccipitals form the considerable portion of the occiput and enclose the foramen magnum laterally and dorsally, separating the supraoccipital from the foramen (Fig. 5A, C). The exoccipitals are transversely divided into a large upper portion and a small lower portion. The upper portion is noticeably convex along its dorsal margin. The healed paraoccipital

process is stout and extends laterally to reach the posterolateral-most portion of the squamosal. The lower portion is inset from the surface of the bone; it is dorsoventrally narrow and lateromedially short. Laterally, the lower and upper portions of the exoccipital form the medial, dorsal, and ventral margins of the cranio-quadrate foramen. Medially, the lower portion dorsoventrally broadens and bears three foramina lateral to the foramen magnum and one foramen ventrolateral the occipital condyle. The dorsal-most foramen in occipital view is the largest and identified as for the exit of skull nerve XII. The two closely positioned and slightly lateral and anterior to the former are the exits of skull nerves IX to XI. The one ventrolateral to the condyle is for the exit of the internal carotid artery. Sutures of the exoccipital with surrounding bones (the squamosal, supraoccipital, basioccipital, and quadrate) are clearly marked.

The basioccipital is incomplete, especially the condyle (Fig. 5A, C). The condyle was heavily damaged, although it is certain that its slightly concave dorsal surface forms the floor of the braincase chamber. The plate portion is nearly vertical, and its posterior surface is weakly concave, showing a well-marked median ridge from the base of the plate down to the margin of the median exit of the Eustachian tube. The vertical plate slightly broadens first and then gradually narrows ventrally. It encloses the posteromedial margin of the lateral exit in addition to the posterior margin of the median exit of the Eustachian tube.

The basisphenoid is exposed limitedly. It is exposed between the pterygoid-quadrate connection and the basioccipital in lateral view and between the pterygoid and basioccipital in occipital view (Fig. 5A, C). It forms the anterolateral margin of the lateral exit and the anterior margin of the medial exit of the Eustachian tube.

Morphological features are not available for the laterosphenoid and prootic due to the coverage of matrix.

Mandibular elements: The left ramus of the mandible is nearly complete and the damaged part of its posterodorsal end can be replenished by the right ramus (Figs. 3A, B; 4; 5C, E). All the bones comprising the mandible are well-exposed in lateral view but limited in medial view because the mandible is tightly occluded with the skull.

The dentary is complete, being anteriorly shallow and posteriorly deep (Figs. 3A, B; 4A, B). The dentaries form the entire symphysis as in *Jiangxisuchus nankangensis* and *Orientalosuchus naduongensis*. The symphysis most likely reaches to the level of the sixth dentary tooth posteriorly. The dentary is broadest across the fourth dentary teeth in ventral view and the symphyseal portion seems to be dorsoventrally shallow. In lateral view, the dental margin is strongly concavo-convex as is the upper jaw and the posterior margin (suture) with the angular is concavo-convex, forming the anterior edge of the external mandibular fenestra dorsally. The posterodorsal suture with the surangular is gently convex toward the latter.

Both splenials are nearly complete except for the posterior ends (Fig. 4A, B). In medial view, the bone is anteriorly narrow and posteriorly broad (Fig. S2C in the online supplementary data). It does not join the formation of the mandibular symphysis anteriorly and its anterior end is forked, with the ventral fork longer than the dorsal one (Fig. S2D, E in the online supplementary data). This feature is similarly present only in *Jiangxisuchus nankangensis* among the known orientalosuchines where the splenial is complete, but the anterior end is much more deeply forked in the latter (Li et al., 2019: fig. 6E, F). There is not any foramen on the medial surface of the splenial body. Posterodorsally, the splenial-coronoid suture is not exposed. Posteroventrally, the splenial encloses the anterodorsal border of the foramen intermandibularis

caudalis, which is large and elliptical as in *Orientalosuchus naduongensis* and *Dongnanosuchus hsui*. The splenial-dentary suture is nearly straight and the right splenial is detached nearly along its total length.

The left surangular is nearly complete (Figs. 3A, B; 4C, D), and its missing part that joins the formation of the retroarticular process is complete in the right one (Fig. 2A, B). In lateral view, the surangular forms the upper half of the posterior part of the mandible. Anteriorly, two processes are nearly equal in length and the dorsal/medial one borders the dentary tooth row lingually as in in *Jiangxisuchus nankangensis*. However, the dorsal one is differently much longer than the ventral/lateral one in the latter species (Li et al., 2019: fig. 6G, H), *Orientalosuchus naduongensis* (Massonne et al., 2019: fig. 9A, B), and *Krabisuchus siamogallicus* (Martin and Lauprasert, 2010: fig. 2C, D). Posterodorsally, the surangular thickens and is not ornamented (Fig. 4C, D). Posteriorly, the surangular narrows considerably posterior to the mandibular glenoid and tapers into a laterally unornamented sharp process that extends nearly to the end of the retroarticular process (Fig. 5A, B). The lateral surangular–angular suture is gently convex towards the angular. Medially, the surangular–angular suture meets the articular nearly at the ventral end and the surangular-articular suture is simply straight (Fig. 5B, D).

The left angular is nearly complete, forming the posteroventral part of the mandible (Figs. 3A, B; 4). Its posteroventral portion is unornamented and narrows into a process, extending to the posterior end of the retroarticular process. As is the case for the surangular, the unornamented region at the posterior-most end served for the insertion of the m. pterygoideus posterior as in extant forms. Anteriorly, the bone forms the posteroventral margin of the external mandibular fenestra where it becomes dorso-ventrally deepest; and it abruptly tapers into a process underlying the dentary further anteriorly. In medial view, the anteroventral end of the

505 angular is forked, forming the posteroventral border of the foramen intermandibularis caudalis
506 (Fig. S2C in the online supplementary data). The relationship of the angular with the coronoid
507 posterodorsal to the foramen is unknown due to the tight occlusion of the mandible with the
508 skull. In medial view, the anterior part of the angular rises to form the medial wall of the deep
509 adductor chamber (Fig. 5B, D).

510 Both articulars are nearly complete, the retroarticular process of the right and the anterior
511 part of the left are better preserved (Figs. 2A, B; Fig. 5B, D). In dorsal view, the retroarticular
512 process is fully exposed. It is roughly triangular in outline and narrows into a ball-shaped end
513 posteriorly. The dorsal surface of the process is deeply concave, with a week but broad
514 prominence along the length of the process (Fig. 4C, D). The foramen aërum usually present at
515 the extreme lingual margin or in from the margin of the retroarticular process in crocodylians is
516 obscured due to fractures. The ventral surface of the retroarticular process is ached and deeply
517 troughed (Fig. 4A, B). The glenoid portion is the broadest part of the bone and about 17 mm in
518 length. The anterior part extends anteroventrally against the medial surfaces of the angular and
519 surangular while slightly narrowing mediolaterally. Both the dorsal and medial surfaces of the
520 anterior part are slightly concave. As mentioned earlier, the sutures of the articular with
521 surrounding bones are very clear.

522 The coronoid is not visible due to the tight occlusion of the mandible with the skull.

523 *Dentition*: The dentition of the left premaxilla is complete, bearing five teeth (Fig. 6A).
524 Of the five teeth, the 5^{th} is the smallest, the 1^{st} and 2^{nd} are nearly same in size and slightly larger
525 than the 5^{th}. The 3^{rd} and 4^{th} teeth are comparable in size, being much larger than the other three
526 (Fig. S1C in the online supplementary data). The labiolingually flattened crowns of the
527 premaxillary teeth are divided by weak carinae that have no serrations. The labial surface is

528 convex, and the lingual surface is concave. There are some subdued striations on the labial
529 surface, converging towards the distal apex.

530 The complete dentition of the maxilla consists of 14 teeth based on the preserved on both
531 sides. The 7th tooth of the left maxilla is missing and the posterior-most two teeth of the right
532 maxilla are obscured by the occlusion of the mandible with the skull. The 1st maxillary tooth is
533 the smallest, even slightly smaller than the 5th premaxillary tooth (Fig. 6C). The teeth posterior to
534 the first enlarges quickly untill to the huge, caniniform 5th tooth; the latter with a crown about 22
535 mm long and 8.5 mm wide at the base as well as convex anterior edge and concave posterior
536 margin. The 6th is slightly larger than the 7th and both are much smaller than the 5th caniniform,
537 even smaller than the 4th tooth (Fig. 6C, D). The 8th tooth is comparable to the 7th in size, but the
538 former is weaky necked at the base (Fig. 6E). The teeth posterior to the 8th are all necked. The 8th
539 to 11th teeth is similar in shape but they become lager and lager in size posteriorly. The crowns of
540 the 12th to 14th teeth are strongly necked at the base and bulb-shaped in lateral view and their
541 sizes decrease posteriorly so that the last (14th) appears around half the 11th in size (Fig. 6F). The
542 anterior teeth that are not constructed or necked at the base are comparable to the premaxillary
543 teeth in morphology. Those teeth with necked base are much less labiolingually flattened and
544 their labial and lingual surfaces are not well divided, and the posterior teeth with bulb-shaped
545 crown may have had a cross-section nearly round.

546 The dentary dentition is extensively covered by the upper jaw (Fig. 3A, B). Anteriorly, a
547 large caniniform tooth fitting into the premaxillary-maxillary notch is identified as the 4th dentary
548 tooth (Fig. 6B), which is the case in other orientalosuchines such as *Dongnanosuchus hsui* and
549 *Orientalosuchus naduongensis*. The crown of the 4th caniniform is comparable to that of the 5th
550 maxillary tooth in both length and basal width and it is also recurved lingually and slightly

551 posteriorly. Among the other dentary teeth, a tooth at the peak of the second dental wave is
552 slightly smaller than the 4th tooth and it is identified as the 12th dentary tooth as in *Jiangxisuchus*
553 *nankangensis*. The distal tip of this tooth fits into a pit of the maxilla between the 7th and 8th
554 maxillary teeth (Fig. 6D, E). In addition, the basal parts of the posterior five teeth are visible on
555 left side in lateral view (Fig. 6F). Their sizes are comparable to those of the correlated teeth of
556 the upper jaw, probably indicating a similar morphology as described for the latter earlier.

557 *Vertebral column*: The first 16 vertebrae are preserved although some of them are
558 incomplete. Their centra are strongly procoelous. The atlas is represented by only the right half
559 of the neural arch (Fig. 5A, C, E, F). The half neural arch appears complete and is stacked on the
560 dorsal surface of the transverse flange of the right pterygoid. It shows its medial surface, with a
561 knob-like base that should sit on the anterolateral side of the atlantal centrum and a thin dorsal
562 part to meet its counterparts from the opposite side. The medial surface of the dorsal part is very
563 concave, bearing a short prezygapophysis to receive the proatlas in life. The posterodorsal
564 margin of the neural arch is very concave, bearing a pronounced postzygapophysis as in extant
565 alligators, such as *Alligator sinensis* (Cong et al., 1998: fig. 72B).

566 The axis is also stacked on the dorsal surface of the pterygoid (Fig. 5A, C). The neural
567 arch is extensively damaged so that the neural canal is dorsally open (Figs. 5E, F; S3A, B).
568 Suture between the odontoid process and the axial centrum is obscured due to fusion, indicating
569 that the specimen represents an adult individual (Brochu, 1996). With the odontoid process, the
570 axial centrum is about 2.51 cm long (Table 1). The odontoid process is slightly convex
571 anterodorsally, nearly flat dorsally, and concavo-convex laterally. The knob-like prominence on
572 the anterolateral side of the odontoid process should be the parapophyseal process for the second

573 cervical rib. The axial centrum is laterally concave and posteriorly convex, being typical
574 procoelous. Ventrally, the hypapophysis is pronounced although it is slightly damaged.
575 The 3rd and 4th cervical vertebrae are detached from the preserved section of the vertebral
576 column. The 3rd cervical is nearly complete and its corresponding ribs are still attached (Fig. 7).
577 Its centrum is about 18.1 mm long. Its neural spine is anteroposteriorly narrow, with its distal tip
578 missing. As shown by the cross-section, the posterior margin of the spine is much thicker than
579 the anterior margin and bears a groove. The parapophysis is typically very low, sitting at the
580 anteroventral margin of the centrum and facing ventrolaterally. The diapophysis on the neural
581 arch is short and faces ventrolaterally. The right prezygapophysis is complete and directs
582 anterodorsally and slightly laterally. Both postzygapophyses are incomplete and face
583 ventrolaterally. In lateral view, the centrum is very concave and its suture with the neural arch is
584 visible in places. The ventral surface of the centrum is also concave and bears a weak midline
585 ridge posterior to the pronounced hypapophysis. The 4th cervical is well-preserved, with its
586 neural spine missing (Fig. 8A-H). Its centrum is slightly longer (19.8 mm) than the 3rd and
587 laterally very concave. There is no midline ridge posterior to the pronounced hypapophysis on
588 the ventral surface which is concave. The parapophysis is still low in position, sitting at the
589 anteroventral margin of the centrum and facing ventrolaterally while the diapophysis is relatively
590 longer than that of the 3rd cervical. The preserved base indicates that the neural spine is similarly
591 narrow as in the 3rd cervical. The centra of the two vertebrae are strongly procoelous as in more
592 posterior vertebrae (Figs. 7-9).
593 The articulated vertebral column contains 12 vertebrae from the 5th to the 16th vertebrae
594 including five cervical and dorsal vertebrae when the 9th vertebra is considered as the last
595 cervical as in extant alligators (Fig. 9, Fig. S4 in the online supplementary data). Compared with

596 the 3rd and 4th cervical vertebrae, there are following changes in the 12 vertebrae. The centrum
597 slightly increases in length (see Table 1); the parapophysis gradually moves dorsally and
598 posteriorly until it moves onto the neural arch at the 12th vertebra where it abuts the anterior side
599 of the base of the diapophysis (Fig. 8I, J), and then the two structures get closer and closer until
600 they merge as a single process, the transverse process, in more posterior dorsals; the
601 hypapophysis is present until to the 13th vertebra as in *Alligator sinensis* (see Cong et al., 1998:
602 fig. 74); and the neural spine becomes anteroposteriorly broad in posterior vertebrae (Fig. S3C-F
603 in the online supplementary data), that of the 15th vertebra being much broader than that of the
604 14th and more anterior vertebrae. In contrast, the neural spine becomes anteroposteriorly broad in
605 the 12th vertebra and more posterior vertebrae in *Alligator sinensis*. The dorsal ends of the
606 complete neural spines of the 12 vertebrae all broaden into a table to receive the dorsal
607 osteoderms as in extant forms.

608 *Ribs*. As mentioned earlier, the 3rd cervical bears ribs, of which the left rib is better
609 preserved than the right. The rib is typically tri-headed with the anterior tip of the free anterior
610 process missing and posterior end incomplete (Fig. 7). The capitulum is shorter but thicker than
611 the tuberculum. The rib is laterally convex and medially concave. The 9th cervical rib is elongate
612 and double-headed as in extant alligators such as *Alligator sinensis* (Cong et al., 1998: fig. 82). It
613 is morphologically very similar to the 1st dorsal rib except its shaft that is thinner than that of the
614 latter (Figs. 9, S4). The other dorsal ribs are incomplete, but the tuberculum becomes shorter and
615 shorter until it merges with the capitulum into a single process in the posterior dorsal ribs.

616 *Osteoderms*. There are three kinds of disarticulated osteoderms preserved (Fig. 10A).
617 Many of them are square-shaped and belong to dorsals (Fig. 10B-D). The dorsal surface of the
618 osteoderms bears large and shallow pits and possess a weak keel along the midline. The lateral

and medial sides of the dorsal osteoderms show articular facets for neighbour osteoderms, which indicates there were more than two rows of paramedian dorsal osteoderms. No articular faces occur on the anterior and posterior sides of the dorsal osteoderms, which suggests that the dorsal osteoderms overlap rather than articulate their posterior neighbours. This is also supported by the presence of a flat, unsculptured area along the anterior margin of the dorsal osteoderms. The ventral surface of the dorsal osteoderms is smooth and transversely concave (Fig. 9). Three dorsal osteoderms of *Jiangxisuchus nankangensis* are preserved in ventral view but articular sutures only occur on two rather than four sides (Li et al., 2019: fig. 2), which indicates that *Jiangxisuchus nankangensis* had more than two rows of paramedian dorsal osteoderms that were most probably arranged in the same pattern as seen here. Our examination of a nearly complete osteoderm (IVPP V 2716-7) indicates that the dorsal osteoderms are more than two rows and similarly arranged in *Eoalligator chunyii* based on the presence of a flat, unornamented area along the anterior margin and articular faces only occurring on two sides of the osteoderm (also see Wang et al, 2016: fig. 7G). These features are also true in the preserved dorsal osteoderms of *Krabisuchus siamogallicus* (see Martin and Lauprasert, 2010: fig. 8), demonstrating the presence of multiple rows of the dorsal osteoderms being arrangement similarly in this form. The preserved dorsal osteoderms of *Orientalosuchus naduongensis* are too fragmentary to determine whether the dorsal osteoderms had multiple rows and were arranged differently in this form (Massonne et al., 2019: fig. 20). There are some small and irregular oval osteoderms preserved (Fig. 9), but only one is complete (Fig. 10F). These small osteoderms should cover the lateral side of the body or dorsal side of the limbs as in extant crocodylians such as *Alligator sinensis* (Cong et al., 1998: fig. 4). As shown by the complete oval osteoderm, these small osteoderms are well sculptured and bears a midline ridge. There are three, incomplete ventral osteoderms

642 preserved (Fig. 9). The ventral osteoderms are flat both externally and internally and ornamented
643 with small pits externally and smooth internally (Fig. 10E).

644 *Pectoral girdle*. We believe that the small left pair of the scapula and coracoid belongs to
645 the new orientalosuchine, *Eurycephalosuchus gannanensis* based on the comparable length ratio
646 between the coracoid and the dorsal vertebrae obtained from extant alligators. In *Alligator*
647 *sinensis* for example, the length ratio between the coracoid and the centrum of the 14th vertebra
648 reaches about 1.67 (Cong et al., 1988: figs. 83, 74), which is close to that (about1.62) measured
649 from the small coracoid to the complete 14th vertebra (See Table 1). In contrast, this ratio would
650 reach 2.25 when the big coracoid is compared to the 14th vertebra. As for the length ratio of the
651 coracoid to the skull, it is 0.253 for the small coracoid but 0.353 for the big coracoid. This ratio
652 again supports the above conclusion that the small coracoid with the scapula belongs to the new
653 species because this length ration is comparable to that of *Alligator sinensis*, close to 0.274
654 calculated based on IVPP #27 with a coracoid length of 3.7 cm and a skull length of 13.5 cm
655 (Cong et al., 1998: a table on page 178). It is true that the length ratio of the coracoid to the skull
656 varies with growth in *Alligator sinensis*, but the range of the variation with growth does not
657 exceed 0.03% within a growth series of five individuals with a coracoid length from 3.2 to 5.3
658 cm and a skull length from 12.1 to 18.7 cm (Cong et al., 1998).

659 The scapula and coracoid of the small pair are disarticulated but they are only one
660 centimeter apart from each other (Figs. 9, S5A). The scapula is incomplete, lacking the distal end
661 of its blade, but the preserved portion is relatively broader than the corresponding part of the
662 scapula of the big pair (Fig. 11A, B, E, F). The blade shows a trend to flare distally as in forms
663 such as *Orientalosuchus naduongensis* which has the part preserved. The blade is strongly
664 constricted just dorsal to the acromial crest on the anterolateral margin, with a minimal width of

12.1 mm that is even slightly bigger than 11.3 of the big scapula. The acromial crest is sharp and thin as in other orientalosuchines where it is known, such as *Krabisuchus siamogallicus*. The lateral surface is gently convex but becomes concave posteroventral to the acromial crest. Medially, the scapula is weakly concave. The anterior margin and the ventral third of the posterior margin are very concave. Posteroventrally, the scapular part of the glenoid is slightly concave. The articular facet for the coracoid is posteriorly very thick but anteriorly thin (Fig. 11I). The scapula may have reached a length (height) of about 5.69 cm when it is complete if the length ratio (1.52) of the large scapula to the large coracoid is taken as a basis of comparison.

The small coracoid is nearly complete, with both ends slightly damaged, especially at the posterodistal side in external view (Fig. 11G, H, I). It is slightly different from *Orientalosuchus naduongensis* in which the anterior margin of the bone is more concave. External surface of the small coracoid is convex but its posteroventral surface just distal to the articular facet for the scapula is concave. As in the scapula, the posterior portion of the articular facet between the coracoid and scapula is much thicker than the anterior portion. The coracoid portion of the glenoid is smaller than the scapular portion and its surface is nearly flat. The coracoid foramen is well developed and situates in the anteroventral part of the bone. It appears that the proximal end is clearly broader than the distal end although the latter is incomplete, which contrasts that of *Orientalosuchus naduongensis* in which both ends are similar in breadth (Massonne et al., 2019: fig. 14M, N).

The interclavicle is slightly damaged in places (Figs. 9, S5A). It is elongate, straight, and sword-shaped in outline. The anterior end and mid portion of the bone are slightly broader than other portions as in *Stangerochampsa mccabei* (Wu et al., 1996: fig. 3 in plate 2). It tapers off

into a narrow process posteriorly. Its lateral margins are much thinner than its middle portion throughout its entire length.

Limbs. The left humerus is the only limb bone preserved (Fig. 12). It is nearly complete, about 85.7 mm long. With the deltopectoral crest and the medial condyle of the distal end slightly damaged. The distal end is relatively much narrower than the proximal end even if the medial condyle is complete (Fig. 12A, G). This contrasts the condition seen in alligatorids such as *Stangerochampsa mccabei* where both ends broaden similarly (Wu et al., 1996: figs. 4-7 in plate 2). In other aspects, the humerus is comparable to that of alligatorids including extant alligators such as *Alligator sinensis*, with a well-developed deltopectoral process (see Cong et l., 1998: fig. 84).

Brevirostres von Zittel, 1890 (sensu Brochu, 2003)

Gen et sp. indet.

Fig. 11B-D, F, J.

Specimen. IVPP V 31267. Articulated right pair of scapula and coracoid mixed up with the specimen (IVPP V 31110) of *Eurycephalosuchus gannanensis*.

Locality and horizon. The construction site of QPM at IPST, Zhanggong District of MGC, Jiangxi Province, China; Hekou Formation, Upper Cretaceous (Maastrichtian) (Zuo et al., 1999).

Comments. As mentioned earlier, IVPP V 31267 was treated here as belonging to an individual of another species other than *Eurycephalosuchus gannanensis* in terms of the bigger size and some morphological differences. This may be also supported by another line of evidence, i.e., the

pattern of its preservation. IVPP V 31267 and IVPP V 31110 are preserved a single block of about 40 cm in length. The former is mixed up with the articulated section of the vertebral column of the latter. In detail, IVPP V 31267 is attached to some dorsal osteoderms of IVPP V 31110 rather than to the vertebrae or ribs below (Figs. 9, S4A, S5A), while the scapula of IVPP V 31110 is normal, attaching to the vertebrae or ribs (Fig. S4B in the online supplementary data). Therefore, the articulated right scapula and coracoid of IVPP V 31267 were washed by running water onto the vertebral column of IVPP V 31110 before they were covered by deposits. In taxonomy, IVPP 31267 cannot represent another species of *Eurycephalosuchus* based on comparison with the two extant species of *Alligator*. The scapula is morphologically very similar in the two species (*Alligator mississippiensis* and *Alligator sinensis*), with both sides of the blade being subparallel dorsally (Brochu, 1999: fig. 51F; Cong et al., 1998: fig.83). In contrast, the sides of the scapular blade broadly flares dorsally in *Eurycephalosuchus gannanensis* (IVPP V 31110) but they are subparallel in IVPP V 31267. *Jiangxisuchus nankangensis* was also collected from the formation that yielded IVPP V 31110 and IVPP V 31267. However, this taxon does not have the pectoral elements available for comparison. Therefore, it was difficult to assign IVPP V 31267 to *Jiangxisuchus nankangensis* with any certainty although it cannot be ruled out that IVPP V 31267 might come from an individual of this species. At the present, we'd better identify IVPP V 31267 as an undetermined brevirostrine (see the phylogenetic part below).

Description

The right scapula is only missing the posterodistal portion of its blade (Figs. 11B-D, F; S5B). It is still articulated with the coracoid of the same side. The distal end of the dorsal blade is slightly broadened as in the extant *Alligator sinensis* (Cong et al., 1998: fig. 83) or *Alligator*

mississippiensis (Brochu, 1999: fig. 51F), differing from the much more expanded condition seen in *Eurycephalosuchus gannanensis* (Fig. 11A, E) or in some alligatorids such as *Stangerochampsa mccabei* from the Upper Cretaceous of Alberta (Wu et al., 1996: fig.1, 2 in Plate 2). The blade is less constricted near its base than that of the latter taxa. As in *Eurycephalosuchus gannanensis*, the acromial crest is pronounced. The lateral surface is gently convex and the area posteroventral to the acromial crest is concave as in other alligatoroids.

The right coracoid is complete but full of cracks (Figs. 11C, D, J; S5A, C). It is relatively short when compared with that of the living alligators such as *Alligator sinensis*, i.e., about 2/3 (66% of) the scapular length in the former while at least over 71% of the scapula length in the latter (see Cong et al., 1998: tables on pages 176 and 178). The anterior margin is much less concave than that of *Eurycephalosuchus gannanensis* and *Orientalosuchus naduongensis* or of the living *Alligator sinensis* but the posterior margin distal to the broadened proximal part is slightly convex as in *Eurycephalosuchus gannanensis* and *Orientalosuchus naduongensis* (Massonne et al., 2019: fig. 14M, N). The distal end is evidently narrower than the proximal end as in *Eurycephalosuchus gannanensis*, which is not comparable to that of *Orientalosuchus naduongensis* or the living *Alligator sinensis*, i.e., both ends are similarly broadened in the former and the distal end is even slightly broader than the proximal end in the latter. In external view, the proximal portion, just anterior to the glenoid, is concave while the distal portion is slightly convex. The coracoid foramen is well-developed and situates near the proximal margin of the bone. The coracoid part of the glenoid is smaller than the scapular portion as in *Eurycephalosuchus gannanensis*.

5. Comparison

As suggested by the following phylogenetic analyses, *Eurycephalosuchus gannanensis* is an orientalosuchine so that we compare it with the other taxa of Orientalosuchina first, especially those taxa that have not been compared in the description with the new species, and then with other crocodylians possessing a short snout from the Upper Cretaceous and the Eocene of China.

The orientalosuchine *Eoalligator chunyii* is from the lower Paleocene of the Nanxiong Basin of Guangdong (about 120 km southwest of Shahe Town). *Eurycephalosuchus gannanensis* clearly differs from *Eoalligator chunyii*; in the latter taxon, the premaxillary-maxillary notch is absent, the supratemporal fenestra is evidently rimed, and the parietal contributes to the occipital edge. As described earlier, *Eurycephalosuchus gannanensis* cannot be compared with *Jiangxisuchus nankangensis* in many features, the most striking of them include the short and broad skull profile, unusually short skull table, the exclusion of the skull from the occipital edge, and the entrance of the splenial into the mandibular symphysis. Compared with *Dongnanosuchus hsui* from the Middle Eocene of Maoming, Guangdong (about 650 km southwest of Shahe Town), *Eurycephalosuchus gannanensis* is also very different in that the preorbital ridge is absent, the frontal enters the supratemporal fossa, and the external mandibular fenestra remains in addition to the unusually short and broadened skull. Compared with another Chinese orientalosuchine, *Eurycephalosuchus gannanensis* cannot be referred to *Protoalligator huiningensis* from the Paleocene of Huaining, Anhui (about 570 km northeast of Shahe Town) because the latter has the skull that is much longer than wide, the splenial that does not enter the mandibular symphysis, and the external mandibular fenestra that is longer than deep.

Orientalosuchus naduongensis, the type species of Orientalosuchina, was discovered from the middle to upper Eocene of the Na Duong Basis of Vietnam (about 1,000 km southwest

779 of Shahe Town). Differences of *Eurycephalosuchus gannanensis* from this Vietnam
780 orientalosuchine are very obvious in addition to the unusually broadened skull and the extremely
781 short skull table. For instance, the interfenestral septum is narrower than the interorbital septum,
782 the frontal enters the supratemporal fossa, and the maxilla-palatine suture is sharply V-shaped.
783 *Krabisuchus siamogallicus* was found in the upper or uppermost Eocene of Krabi, Thailand
784 (about 2,600 km southwest to Shahe Town). This orientalosuchine is not complete, but it is
785 clearly different from *Eurycephalosuchus gannanensis* in that interorbital septum is narrower
786 than the interfenestral septum, the frontal is excluded from the supratemporal fossa, the parietal
787 reaches the occipital edge posteriorly, the palatine-pterygoid suture is parallel to the posterior
788 margin of the suborbital fenestra, and the teeth are coarsely striated.

789 In comparison with other short-snouted crocodylians from the Upper Cretaceous-Eocene
790 of China, *Asiatosuchus nanlingensis* (Young, 1964, Wu et al., 2018) collected from the
791 uppermost Cretaceous of the Nanxiong Basin is a fragmentary taxon and has been argued to have
792 a long-snouted species (Wu et al., 2018, figs. 1A, 1C; 2A, 2B) and is clearly not comparable to
793 *Eurycephalosuchus gannanensis*. *Planocrania datangensis* Li, 1976 recovered from the
794 lowermost Paleocene of the Nanxiong Basin has a moderately elongated snout with ziphodont
795 teeth (Brochu, 2013, figs. 10, 11) so that this species evidently differs from *Eurycephalosuchus*
796 *gannanensis*.

797 *Asiatosuchus grangeri* Mook, 1940 from the Upper Eocene of Inner Mongolia has been
798 considered as a basal crocodyloid in many studies, which is confirmed by the phylogenetic
799 analyses presented here. The holotype of this species is a mandible, which differs from that of
800 *Eurycephalosuchus gannanensis* in having a postdentary portion that is relatively much
801 shallower, a splenial that does not enter the symphysis, and an external mandibular fenestra that

802 is horizontally long. Zhang (1981) described *Wanosuchus atresus* based on a left ramus of a
803 mandible from the Paleocene of Anhui Province as a sebecosuchian, which has not been
804 included in any phylogenetic study so far. This species differs from *Eurycephalosuchus*
805 *gannanensis* in that it lacks an external mandibular fenestra and its splenial is excluded from the
806 symphysis. Li and Wang (1987) described *Alligator luicus* based on a skull and some postcranial
807 elements from the Middle Miocene, Shandong Province. The divided external nares, the
808 exclusion of the frontal from the supratemporal fenestra, and the contribution of the parietal to
809 the occipital edge clearly distinguish *Alligator luicus* from *Eurycephalosuchus gannanensis*.
810 *Dzungarisuchus manacensis* Dong, 1974 is represented by a mandibular ramus recovered from
811 the Upper Eocene of Xinjiang and considered a crocodyline. The elongated symphyseal region
812 and same-sized alveoli are not comparable to those of *Eurycephalosuchus gannanensis*.
813
814 **6. Phylogenetic analyses**
815
816 In phylogenetic studies of crocodyloids or alligatoroids, a number of different data matrices
817 have been built up recently. Shan et al. (2021) presented the most recent one in which the
818 phylogenetic relationships of all orientalosuchines then known were comparatively verified by
819 two sets of data matrices that included the new orientalosuchine established in this work.
820 Specifically, the first set of the data matrices of Shan et al. (2021) was employed here because it
821 included more terminal taxa. With the addition of *Eurycephalosuchus gannanensis* and
822 Brevirostres gen. et sp. indet., the data matrix in total comprised 125 terminal taxa and 191
823 morphological characters (see online supplementary data). In this data matrix, there were coding
824 changes in characters resulting from further examination of specimens for *Jiangxisuchus*

825 *nankangensis* (characters 54, 169, and 126), *Dongnanosuchus hsui* (characters 123, 169, and
826 160), and *Eoalligator chunyii* (character 79), respectively; for *Orientalosuchus naduongensis*,
827 the coding change of character 79 was made based on the published figures by Massonne et al.
828 (2019); and for *Bernissatia fagessi*, the coding change of 21 characters were made based on new
829 morphological information provided by the restudy of Martin et al. (2020) on the lectotype
830 specimen (IRSNB R46) (see online supplementary data).

831 It is impossible to assess character states with any confidence for most characters to
832 *Asiatosuchus nanlingensis* because the only available specimen of this species is highly
833 fragmentary; the taxon was therefore excluded in the phylogenetic analysis conducted here, as
834 was the case in recent studies (Li et al. (2019; Massonne et al., 2019; Shan et al., 2021). In
835 addition, Brevirostres gen. et sp. indet. is too fragmentary to be included in the phylogenetic
836 analysis. In the analysis, multistate characters were unordered, and all characters were equally
837 weighted. A New Traditional Search Method of TNT v.1.5 standard version was preferred
838 (Goloboff and Catalano, 2016), with setting the maximum for trees to 10,000 and analyzed using
839 1000 random seeds of tree fusing as in Li et al. (2019) and Shan et al., 2021.

840 The analysis of 123 taxa yielded eight most parsimonious trees (MPTs), each with a tree
841 length of 923 steps, a consistency index (CI) of 0.283, and a retention index (RI) of 0.772. As
842 shown in the strict consensus tree of the eight MPTs (Fig. 13), the analysis recognized
843 *Eurycephalosuchus gannanensis* as an alligatoroid within Orientalosuchina and also suggested
844 the basal position of Orientalosuchina within Globidonta as in Shan et al. (2021). The
845 alligatoroid status of Orientalosuchina was supported by seven unequivocal synapomorphies,
846 including characters 47-0 (alveoli for dentary teeth 3 and 4 nearly same size and confluent), 61-1
847 (anterior processes of surangular subequal to equal),70-1 (foramen aërum set in from margin of

retroarticular process), 104-1 (maxilla broadly separates ectopterygoid from maxillary tooth row), 131-1 (anterior tip of frontal forms broad, complex sutural contact with the nasals), 141-1 (quadratojugal spine high, between posterior and superior angles of infratemporal fenestra), and 177-1 (quadrate foramen aërum on dorsal surface of quadrate). Of the synapomorphies, character 104 could not be determined for *Eurycephalosuchus gannanensis* due to poor preservation, character 47-1 independently developed, and the states of characters 70, 131, and 177 are reversals in the species. The globidontian status of Orientalosuchina was supported by three unequivocal synapomorphies: characters 39-1 (dorsal midline osteoderms nearly square), 47-1 (fourth alveolus larger than third and alveoli are separated), and 150-2 (frontoparietal suture on skull table entirely alveoli for dentary teeth 3 and 4 nearly same size and confluent), of which character 150-1 was hypothesized to be derived from state-0 independently in *Eurycephalosuchus gannanensis*. With the inclusion of *Eurycephalosuchus gannanensis*, the monophyletic Orientalosuchina recognized by Massonne et al. (2019) and Shan et al. (2021) was supported. This was suggested by five unequivocal synapomorphies: characters 64-1 (surangular–dentary suture intersects external mandibular fenestra at posterodorsal corner (1), 70-0 (foramen aërum setting at extreme lingual margin of retroarticular process), 143-0 (postorbital neither contacts quadrate nor quadratojugal medially), 159-1 (squamosal extending ventrolaterally to lateral extent of paraoccipital process), and 160-2 (supraoccipital exposure on dorsal skull table large). Of the five synapomorphies, character 160 is represented by state 3 in *Eurycephalosuchus gannanensis* (supraoccipital exposure on dorsal skull table large such that parietal is excluded from posterior edge of table). Within Orientalosuchina, *Eurycephalosuchus gannanensis* was nested by one unequivocal synapomorphies into a clade with other three Chinese forms and one Vietnam taxon, with an undetermined relationship. The synapomorphy is

871 character 92-1 (an occlusion pit between 7th and 8th maxillary teeth and all other dentary teeth
872 occlude lingually). Nevertheless, the majority-rule consensus of the five MPTs suggested that
873 *Eurycephalosuchus gannanensis* was the sister-group of the *Jiangxisuchus nankangensis*-
874 *Eoalligator chunyii* sub-clade (Fig. S6 in the online supplementary data), which was supported
875 by two synapomorphies: characters 61-0 (anterior processes of surangular unequal) and 150-1
876 (frontoparietal suture makes modest entry into supratemporal fenestra at maturity, postorbital and
877 parietal in broad contact).

878 In the previous studies that also included 'orientalosuchines' based on the known taxa
879 available at the time (*Krabisuchus siamogallicus*, *Eoalligator chunyii*, *Protoalligator*
880 *huiningensis*, and *Jiangxisuchus nankangensis*), the phylogenetic analysis did not demonstrate a
881 monophyletic clade for those 'orientalosuchines' within Alligatoroidea and *Eoalligator chunyii*
882 and *Jiangxisuchus nankangensis* were in fact included in the Crocodyloidea (Matin et al., 2010;
883 Wang et al., 2016, Li et al., 2019). As mentioned earlier, the monophyletic Orientalosuchina was
884 first recognized by Massonne et al. (2019) based on the discovery of *Orientalosuchus*
885 *naduongensis* and was further confirmed by the establishment of *Dongnanosuchus nankangensis*
886 of Shang et al. (2021). Compared with the two studies, the phylogenetic relationships here
887 recovered for the major clades of Eusuchia are different. The most striking of those differences
888 are that the monophyly of Crocodylia was not supported different. The most striking of those
889 differences are that the monophyly of Crocodylia was not supported because its basal most clade
890 (Gavialoidea) formed a polytomy with the two basal clades of Eusuchia (Hylaeochampsidae and
891 Allodaposuchidae) and a clade including all other crocodylians (Fig. 13). As for Alligatoroidea,
892 the phylogenetic results recovered here are much more similar to those obtained by Shan et al.
893 (2021) based on the first data set, i.e., the monophyletic status of the major clades were

894 confirmed and Orientalosuchina was again considered as the basal-most clade of Globidonta
895 within Alligatoroidea. There are only a few differences. For instance, the phylogenetic
896 relationships of *Diplocynodon* and *Deinosuchus* were uncertain, forming a trichotomy with
897 Globidonta and internal relationships within Caimaninae were poorly resolved. In addition,
898 *Bernissatia fagesii* rather than *Theriosuchus pusillus* were hypothesized as the sister group of
899 Eusuchia. For the internal relationships of Orientalosuchina, the phylogenetic results obtained
900 here are also comparable to those of Shan et al. (2021), with *Krabisuchus siamogallicus* and
901 *Protoalligator huiningensis* recognized as two successive taxa at the base of the clade and the
902 new species *Eurycephalosuchus gannanensis*, *Orientalosuchus naduongensis*, and
903 *Dongnanosuchus nankangensis* forming a polytomy with *Jiangxisuchus nankangensis*-
904 *Eoalligator chunyii* clade.
905 In order to determine the taxonomic status of Brevirostres get. et sp. indet. (IVPP V
906 31267), we included it in a phylogenetic analysis with the same setting as in the previous one.
907 The analysis produced seven MPTs. As displayed by the strict consensus of the seven MPTs,
908 internal relationships obtained by the previous analysis for the taxa of Brevirostres were
909 extensively collapsed and IVPP V 31267 could not be phylogenetically grouped with any other
910 taxon but was just recognized as a brevirostrine (see Fig. S7 in the online supplementary data),
911 representing an undetermined brevirostrine.
912

913 ## 7. Discussion

914

915 *Eurycephalosuchus gannanensis* appears to be the smallest in size among the
916 orientalosuchines based on the skull length; it is slightly smaller than *Krabisuchus siamogallicus*

based on the skull length or than *Eoalligator chunyii* in terms of the width of the occiput. However, as argued earlier, morphological differences between *Eurycephalosuchus gannanensis* and the other orientalosuchines are obvious. Brevirostres gen. et sp. indet. should be a medium-sized animal as suggested by the length (5.23 cm) of its complete coracoid, which is about 135% larger than that of *Eurycephalosuchus gannanensis* and nearly same to that (5.2) of a specimen (IVPP #27) of *Alligator sinensis* (see Cong et al., 1998: the table on page 178). The skull of IVPP #27 is 18.06 cm long (see Cong et al., 1998: table 2).

In Orientalosuchina, the phylogenetic analysis conducted here not only supported the monophyly of Orientalosuchina but also confirmed the phylogenetic pattern obtained by Shan et al. (2021) for the previous six orientalosuchines. As suggested by the majority rule consensus tree, *Eurycephalosuchus gannanensis* may have been closely related to *the Jiangxisuchus nankangensis-Eoalligator chunyii* clade, which is in accordance with their paleogeographical and stratigraphical occurrence, i.e., they were all recovered from the Upper Cretaceous (Maastrichtian) red beds of Ganzhou and Nanxiong, the latter is about 105 km apart in the southwest. Although the relationships among Orientalosuchina and the major clades of Alligatoroidea were resolved, most of them had a very low Bremer support value for monophyly, i.e., with a value of 1 or 0 as in Massonne et al. (2019) and Shan et al. (2021). On the other hand, in all previous studies with the Chinese orientalosuchines included, monophyly of the major groups of the Crocodylia were also weakly supported (Wang et al., 2016; Li et al., 2019). It would not be surprising that such relationships demonstrated in our study and others would change when novel taxa and new, more complete specimens of the species currently only known from fragmentary remains are found. As mentioned in Li et al. (2019) and Shan et al. (2021), there were a number of short-snouted fossil members of Crocodylia collected from the Upper

940 Cretaceous to Eocene in China before the discovery of *Eurycephalosuchus gannanensis*. In
941 addition to those mentioned earlier, they also include *Dzungarisuchus manacensis* from the
942 upper Eocene of Manas River, Xinjiang and *Lianghusuchus hengyangensis* Young, 1948 from
943 the Eocene of Hengyang, Hunan. However, none of them is as well-preserved as the Chinese
944 orientalosuchines such as *Dongnanosuchus hsui*, *Jiangxisuchus nankangensis*, or
945 *Eurycephalosuchus gannanensis*. Additionally, many of the Chinese crocodylians have not been
946 included in phylogenetic studies because most of them are fragmentary and their taxonomic
947 status requires revision using modern technics and methods.

948 Our phylogenetic analysis did not support the phylogenetic relationships obtained by
949 previous studies (such as Narváez et al., 2016, Massonne et al., 2019, Shan et al., 2021) for two
950 basal clades of Eusuchia and Gavialoidea (the basal most clade of Crocodylia), this was likely
951 caused by the addition of new morphological information to *Bernissartia fagesii* which was
952 newly recovered by Martin et al. (2020).

953 Our phylogenetic analysis further supported that Orientalosuchina represents an independent
954 clade with no close relationship to any of the North American alligatoroids; it deviated from the
955 main line of Alligatoroidea. As mentioned above, it is uncertain whether the deviation took place
956 after *Diplocynodon* in Europe or *Deinosuchus* in North America during the late Cretaceous.
957 However, it was further supported that Orientalosuchina split from the Alligatoridae and
958 dispersed to Asia through only one divergence event as early as the Campanian. Such a dispersal
959 event again refuses the views that Orientalosuchina formed a sub-lineage with some of the North
960 American alligatoroids and that it dispersed to Asia from North America after at least four
961 divergence events occurred within the sub-lineage during the Late Cretaceous. This would mean
962 that Orientalosuchina had no close relationship with the Alligatoridae in terms of either

963 phylogeny or dispersal pattern. Although, as discussed earlier, the phylogenetic results obtained
964 here are only weakly supported as in previous studies, the similar view reflected by the
965 successive studies of *Dongnanosuchus hsui* and *Eurycephalosuchus gannanensis* from China for
966 the origin and dispersal hypotheses of Orientalosuchina and the later alligatoroid clades may
967 have likely represented the true situation. Of course, this needs to be further verified by future
968 studies with new information.

969 The specimen (a pair of the scapula and coracoid) of Brevirostres gen. et sp. indet. were
970 preserved together with that of *Eurycephalosuchus gannanensis*, but it is impossible to determine
971 the precise spatial extent of the two species. However, the relative completeness of individual
972 elements of both specimens indicates the possibility of a range overlap and coexistence between
973 these species during the earliest stage of the Maastrichtian in the region. Additional specimens of
974 both species from the region would solidify these observations. Sympatric crocodyliforms are a
975 common occurrence both throughout their fossil record (Bryant 1989, Riff et al. 2010, Scheyer et
976 al. 2013, Moreno-Bernal et al. 2016) and in the present day (Campos & Magnusson 2013,
977 Choudhary et al 2018). As such, range overlap and ecological interactions between the two
978 species of brevirostrines would not be particularly surprised. Taking reference to modern
979 crocodylians, possibilities in terms of environmental tolerances, habitat requirements, and/or
980 behaviors may have been present with two species. Morphological features of the skull
981 indicating prey preference is a common means of determining ecological partitioning between
982 fossil crocodyliforms. This does not appear to be useful in this case due to the absence of the
983 skull in Brevirostres gen. et sp. indet. Campos and Magnusson (2013) observed that the dwarf
984 caiman *Paleosuchus palpebrosus* tolerates cooler temperatures, which helps it to occupy areas
985 not hospitable to its sympatric peers. Similarly, Choudhary et al. (2018) reported that the

sympatric crocodylians (*Crocodylus palustris* and *Gavialis gangeticus*) demonstrate references in basking site substrate type, water depth and gradient, and nesting sites. Considering the larger size, Brevirostres gen. et sp. indet. may have dominated the region and had a wider range of preying. To investigate any one of these possibilities needs further data, finding new specimens of both species.

Conclusions

The distinctive skull morphology of the new crocodylian specimens plays a key role in the establishment of a new orientalosuchine, *Eurycephalosuchus gannanensis* and the evidently large size and morphological differences of an articulated scapula and coracoid suggest the presence of another, undeterminable species of Brevirostres in the same region. Our phylogenetic analysis incorporating the new form *Eurycephalosuchus gannanensis* supports the monophyly of Orientalosuchina and that the clade is the sister-group of the Alligatoridae and dispersed into Asia after a divergence event occurred in the mainline rather than after multiple divergence events in a sub-lineage of the Alligatoroidea during the Late Cretaceous. It will be fundamental to find more taxa and better specimens of species currently only known from fragmentary material in establishing a stable phylogenetic pattern for Alligatoroidea as well as in improving hypotheses on the early history and dispersal routes of alligatoroid clades between continents. Sympatric relationship of *Eurycephalosuchus* with an undeterminable brevirostrine is uncertain currently based on available information.

Acknowledgments

We are grateful to Fang Zheng and Wei Zhang of Institute of Vertebrate Paleontology and Paleoanthropology (IVPP), Chinese Academy of Sciences, Beijing for their work on 3D scanning and 3D cast of the specimen. We thank Wei Gao of IVPP for taking photographs of the specimens used in the paper. We appreciate two anonymous reviewers who carefully examined the manuscript, offering critical comments and suggestions that led to its great improvement. This project is supported by Research grants from Canadian Museum of Nature (RCP09 to X.-C. Wu) and from the Strategic Priority Research Program of the Chinese Academy of Sciences (XDB26000000 to H.-L You) and National Natural Science Foundation of China (41688103, 41872021 to H.-L You). We appreciated the assistance of the Willi Hennig Society through providing access to the software TNT 1.5.

References

Benton, M.J., Clark, J.M., 1988. Archosaur phylogeny and the relationships of the Crocodylia. In: Benton, M.J. (Ed.), The phylogeny and classification of the tetrapods, Systematics Association Special Vol. 35A. Clarendon Press, Oxford, 295–338.

Brochu, C.A., 1996. Closure of neurocentral sutures during crocodilian ontogeny: implications for maturity assessment in fossil archosaurs. Journal of Vertebrate Paleontology 16(1), 49–62.

Brochu, C.A., 1999, Phylogenetics, taxonomy, and historical biogeography of Alligatoroidea, *in* Rowe, T., Brochu, C.A., and Koshi, K., eds., Skull morphology of *Alligator*

mississippiensis and phylogeny of Alligatoroidea: Society of Vertebrate Paleontology, Memoir 6, 9–100.

Brochu, C.A., 2003, Phylogenetic approaches toward crocodylian history: Annual Review of Earth and Planetary Sciences 31, 357–397.

Brochu, C., 2013, Phylogenetic relationships of Palaeogene ziphodont eusuchians and the status of *Pristichampsus* Gervais, 1853: Earth and Environmental Science Transactions of the Royal Society of Edinburgh 103, 521–550.

Bryant, L.J. 1989, Non-dinosaurian lower vertebrates across the Cretaceous-Tertiary boundary in northeastern Montana: University of California Publications in Geological Sciences 134, 25–43.

Campos, Z., Magnusson, W.E., 2013. Thermal relations of dwarf caiman, *Paleosuchus palpebrosus*, in a hillside stream: Evidence for an unusual thermal niche among crocodilians. Journal of Thermal Biology 36, 20–23. https://doi.org/10.1016/j.jtherbio.2012.09.004.

Cheng, Y.-N., Ji, Q., Wu, X.-C., Shan, H.-Y., 2008, Oviraptorosaurian Eggs (Dinosauria) with embryonic skeletons discovered for the first time in China. Acta Geologica Sinica 82, 1089–1094.

Choudhary, S., Choudhary, B.C., Gopi, G.V., 2018. Crocodilians (Gavialis gangeticus & Crocodylus palustris) in Katarniaghat Wildlife Sanctuary, India. Aquatic Conservation Marine and Freshwater Ecosystems 2018, 1–10. https://doi.10.1002/aqc2911.

Cong, L.-Y., Hou, L.-H., Wu, X.-C., Hou, J.-F., 1998. The gross anatomy of *Alligator sinensis* Fauvel. Science Press, Beijing. [In Chinese, with English summary].

Dong, Z.M., 1974. The crocodile fossils from Xinjiang. Vertebrata PalAsiatica 12, 187–188. [in Chinese with English summary]

Goloboff, P.A., and Catalano, S.A., 2016. TNT version 1.5, including a full implementation of phylogenetic morphometrics. Cladistics 32, 221–238. https://doi:0.1111/cla.12160.

Gmelin, J.F., 1789. Caroli a Linné Systema Naturae per Regna Tria Naturae, Secundum Classes, Ordines, Genera, Species, cum Characteribus, Differentiis, Synonymis, Locis, Tomus 1, Pars 2, Editio Decima Tertia, Aucta, Reformata. Leipzig, Georg Emanuel Beer.

Gray, J.E., 1844. Catalogue of the tortoises, crocodiles, and amphisbaenians in the collection of the British Museum: British Museum, London.

He, F.-l., Huang, X.-j., Li, X.-y., 2017. Occurrence rule and buried characteristics of dinosaur fossils in the Ganzhou Basin, Jiangxi Province. East China Geology 38, 250–254. https://doi:10.16788/j.hddz.32-1865/P.2017.04.002.

Huxley, T.H., 1875. On the clasificación of the Animal Kingdom: Journal of the Linnean Society of London, Zoology 12, 199–226.

Iordansky, N.N., 1973. The skull of the Crocodylia. In: Gans, C. and Parson, T.S. (eds.), Biology of the Reptilia. Academic Press, New York, 201–262.

Jiangxi Bureau of Geology and Mineral Resources, 1984. Regional geology of Jiangxi Province. Geological Publishing House, Beijing. [In Chinese].

Li, C., Wu, X.-C., Rufolo, S.J., 2019. A new crocodyloid (Eusuchia: Crocodylia) from the Upper Cretaceous of China. Cretaceous Research 94, 25–39. https://doi.org/10.1016/j.cretres.2018.09.015.

Li, J., 1976. A sebecosuchian found from the Nanxiong Basin, Guangdong. Vertebrata PalAsiatica 14, 169–173. [In Chinese]

1076 Li, J., Wang, B.-Z., 1987. A new species of Alligator from Shanwang, Shandong: Vertebrata
1077 PalAsiatica 7, 199–207. [in Chinese with English abstract]
1078 Lü, I., Yi, L., Zhong, H., Wei, X., 2013a. A New somphospondylan sauropod (Dinosauria,
1079 Titanosauriformes) from the Late Cretaceous of Ganzhou, Jiangxi Province of Southern
1080 China. Acta Geologica Sinica 87, 678–685.
1081 Lü, I., Yi, L., Zhong, H., Wei, X., 2013b. A new oviraptorosaur (Dinosauria: Oviraptorosauria)
1082 from the Late Cretaceous of Southern China and its paleoecological Implications. PLoS
1083 ONE 8(11), e80557. https//doi:10.1371/journal.pone.0080557.
1084 Lü, J., Yi, L., Brusatte, S.L., Yang, L., Li, H., Chen, L., 2014. A new clade of Asian Late
1085 Cretaceous long-snouted tyrannosaurids. Nature Communications 5, 3788.
1086 https://doi.org/10.1038/ncomms4788.
1087 Lü, J., Pu, H., Kobayashi, Y., Xu, L., Chang, H., Shang, Y., Liu, D., Lee, Y.-N, Kundrát, M.
1088 Shen, C., 2015. A New Oviraptorid Dinosaur (Dinosauria: Oviraptorosauria) from the
1089 Late Cretaceous of Southern China and Its Paleobiogeographical Implications. Scientific
1090 Reports 5, 11490. https://doi:10.1038/srep11490.
1091 Lü, J., Chen, R., Brusatte, S.L., Zhu, Y., Shen, C., 2016. A Late Cretaceous diversification of
1092 Asian oviraptorid dinosaurs: evidence from a new species preserved in an unusual
1093 posture. Scientific Reports 6, 35780. https://doi:10.1038/srep35780.
1094 Lü, J., Li, G., Kundrát, M., Lee, Y., Sun, Z., Yoshitsugu, K., Sun, C., Teng, F., Liu, H., 2017.
1095 High diversity of the Ganzhou Oviraptorid Fauna increased by a new cassowary-like
1096 crested species. Scientific Reports 7, 6393. https://doi:10.1038/s41598-017-05016-6.

1097 Martin, J.E., Lauprasert, K., 2010. A new primitive alligatorine from the Eocene of Thailand:
1098 relevance of Asiatic members to the radiation of the group. Zoological Journal of the
1099 Linnean Society 158(3), 608–628. https://doi: 10.1111/j.1096-3642.2009.00582.x.
1100 Martin, J.E., Smith, T., Salaviale, C., Adrien, J. and Delfino, M., 2020. Virtual reconstruction of
1101 the skull of Bernissartia fagesii and current understanding of the neosuchian-eusuchian
1102 transition. Journal of Systematic Palaeontology 18(13), 1079–1101.
1103 Massonne, T., Vasilyan, D., Rabi1, M., Böhme, M., 2019. A new alligatoroid from the Eocene of
1104 Vietnam highlights an extinct Asian clade independent from extant *Alligator sinensis*.
1105 PeerJ 7, e7562. hppts://doi:10.7717/peerj.7562.
1106 Mo, J.-Y., Xu, X., Evans S.E., 2010. The evolution of the lepidosaurian lower temporal bar: new
1107 perspectives from the Late Cretaceous of South China. Proceedings of the Royal Society
1108 B 277, 331–336.
1109 Mo, J.-Y., Xu, X., Evans, S.E., 2012. A large predatory lizard (Platynota, Squamata) from the
1110 Late Cretaceous of South China. Journal of Systematic Palaeontology 10, 333–339.
1111 http://dx.doi.org/10.1080/14772019.2011.588254.
1112 Mook, C.C., 1940. A new fossil crocodilian from Mongolia. American Museum of Natural
1113 History Novitates 1097, 1–3.
1114 Moreno-Bernal, J.W., Head, J., Jaramillo, C.A., 2016. Fossil Crocodilians from the High Guajira
1115 Peninsula of Colombia: Neogene faunal change in northernmost South America. Journal
1116 of Vertebrate Paleontology 36(3), e1110586.
1117 https://doi:10.1080/02724634.2016.1110586.
1118 Narváez, A., Brochu, C.A., Escaso, B.F., Perez-García, A., Ortega, F., 2016. A New Spanish
1119 Late Cretaceous eusuchian reveals the synchronic and sympatric presence of two

allodaposuchids. Cretaceous Research 65, 112–125. http://dx.doi.org/10.1016/j.cretres.2016.04.018.

Riff, D., Romano, P.S.R., Oliveira, G.R., Aguilera, O.A., 2010. Neogene crocodile and turtle fauna in northern South America. Amazonia, Landscape and Species Evolution: A Look into the Past 3, 259–280. https://doi:10.1002/9781444306408.ch16.

Sato, T., Cheng, Y.-n., Wu, X.-C., Zelenitsky, D.K., Hsiao, Y.-f., 2005. A pair of shelled eggs inside a female dinosaur. Science 308 (5720), 375.

Scheyer, T.M., Aguilera, O.A., Delfino, M., Fortier, D.C., Carlini, A.A., Sánchez, R., Carrillo Briceño, J.D., Quiroz, L., Sánchez-Villagra, M.R., 2013. Crocodylian diversity peak and extinction in the late Cenozoic of the northern Neotropics. Nature Communications 4(1970), 1–9. https://doi:10.1038/ncomms2940.

Shan, H.-Y., Wu, X.-C., Cheng, Y.-N., Sato, T., 2017. Maomingosuchus petrolica, a restudy of '*Tomistoma' petrolica* Yeh, 1958. Palaeoworld 26, 672–690.

Shan, H.-Y., Wu, X.-C., Sato, T., Cheng, Y.-N., Rufolo, S.J., 2021. A new alligatoroid (Eusuchia, Crocodylia) from the Eocene of China and its implications for the relationships of Orientalosuchina. Journal of Paleontology 95, 1321–1339. https//doi.org/1o.1017/jpa.2021.69.

Tong, H.-Y., Mo, J.-Y., 2010. *Jiangxichelys*, a new nanhsiungchelyid turtle from the Late Cretaceous of Ganzhou, Jiangxi Province, China: Geological Magazine 147, 981-986.

Wang, S., Sun, C., Sullivan, C., Xu, X., 2013. A new oviraptorid (Dinosauria: Theropoda) from the Upper Cretaceous of southern China. Zootaxa 3640, 242–257.

Wei, X.-F., Pu, H.-Y., Xu, L., Liu, D., Lü, J.-C., 2013. A new oviraptorid dinosaur (Theropoda: Oviraptorosauria) from the Late Cretaceous of Jiangxi Province, southern China. Acta Geologica Sinica 87, 899–904.

Wen, C., Liu, X., Lü, B., Mao, X., Chen, J., Hou, S., Zhou, Z., Hou, J., Wu, H., 2016. The Cretaceous redbeds in Shicheng Basin, Jiangxi province: pedogenic and paleoenvironmental characteristics. Quaternary Science 36, 1403–16.

Wang, Y.-Y., Sullivan, K., and Liu, J., 2016, Taxonomic revision of *Eoalligator* (Crocodylia, Brevirostres) and the paleogeographic origins of the Chinese alligatoroids. PeerJ 4, e2356. https//doi:10. 7717/peerj.2356.

Wu, X.-C., Brinkman, D.B., Russel, A.P., 1996. A new alligator from the Upper Cretaceous of Canada and the relationships of early eusuchians. Palaeontology 39, 351–375.

Wu, X.- C., Russell, A.P., Brinkman, D.B., 2001. A review of *Leidyosuchus canadensis* Lambe, 1907 (Archosauria: Crocodylia) and an assessment of skull variation based upon new material. Canadian Journal of Earth Sciences 38, 1665–1687.

Wu, X.-C., Li, C., Wang, Y.-Y., 2018. Taxonomic revision and phylogenetic test of *Asiatosuchus nanlingensis* Young, 1964 and *Eoalligator chunyii* Young, 1964. Vertebrata PalAsiatica 56, 137–146.

Xing, L., Niu, K., Wang, D., Marquez, A.P., 2020a. A partial articulated hadrosaurid skeleton from the Maastrichtian (Upper Cretaceous) of the Ganzhou area, Jiangxi Province, China. Historical Biology 32, 2256–2259. https://doi.org/10.1080/08912963.2020.1782397.

Xing, L., Niu, K., Zhang, L., Yang, T.-R., Zhang, J., Persons IV, W.S., Romilio, A., Zhuang, Y., Ran, Y., 2020b. Dinosaur Eggs Associated with Crustacean Trace Fossils from the Upper

Cretaceous of Jiangxi, China: Evidence for Foraging Behavior? Biosis. Biological Systems 1(2), 54–59. https://doi.org/10.37819/biosis.001.002.0058.

Xing, L., Niu, K., Ma, W., Zelenitsky, D.K., Yang, T.-R., Brusatte, S.L., 2021. An exquisitely preserved *in-ovo* theropod dinosaur embryo sheds light on avian-like prehatching postures. iScience 103516. https://doi.org/10.1016/.

Xu, X., Han, F.-L., 2010. A new oviraptorid dinosaur (Theropoda: Oviraptorosauria) from the Upper Cretaceous of China. Vertebrata PalAsiatica 48, 11–18.

Young, C. C., 1948, Fossil crocodiles in China, with notes on dinosaurian remains associated with the Kansu crocodiles: Bulletin of Geological Society of China 28, 255–288.

Young, C. C., 1964, New fossil crocodiles from China: Vertebrata PalAsiatica, v. 5, p. 189–208.

Young, C. C., 1982, A Cenozoic crocodile from Huaining, Anhui: *in* Selected Works of Yang Zhongjian: Beijing, Science Press, 47–48.

Zhang, F.-K., 1981, A fossil crocodile from Anhui Provine: Vertebrada PalAsiatica 19, 200–207. [in Chinese with English abstract]

von Zittel, K.A. 1890. Handbuch der Paläontologie, Vol. 3. Vertebrata (Pisces, Amphibia, Reptilia, Aves). Oldenbourg, Munich.

Zuo, Y., Wu, J., Zhou, W., 1999. Lithostratigraphic division of volcanic terrain in Late Mesozoic in Jiangxi. Geological Review 45, 742–750.

Figures and Figure Captions

Figure 1. Schematic maps depicting fossil localities of *Eurycephalosuchus gannanensis* gen. and sp. nov. and other orientalosuchines. A, main part of China; B, Jiangxi Province and parts of Anhui and Guangdong Provinces, showing the fossil localities of some Chinese orientalosuchines. C, relative distances among the fossil localities of orientalosuchines (1 = *Dongnanosuchus hsui*, Maoming Basin, Guangdong; 2 = *Eoalligator chunyii*, Nanxiong Basin, Guangdong Province; 3 = *Jiangxisuchus nankangensis*, *Eurycephalosuchus gannanensis* gen. et sp. nov., and *Eurycephalosuchus* sp. indet., Ganzhou Basin, Jiangxi Province; 4 = *Protoalligator huiningensis*, Huaining, Anhui Province; 5 = *Orientalosuchus naduongensis*, Vietnam; 6 = *Krabisuchus siamogallicus*, Thailand). N = north. **Page-size**

Figure 2. Photographs and corresponding line drawings of skull of *Eurycephalosuchus gannanensis* gen. and sp. nov. A and B, skull in dorsal view; C and D, posterior part of skull table in dorsal and slightly posterior views, showing relationships between quadrate and its neighboring bones in supratemporal fossa. Zigzag lines indicate a broken surface. Abbreviations as listed in the text. **Page-size**

Figure 3. Photographs and corresponding line drawings of skull and mandible of *Eurycephalosuchus gannanensis* gen. and sp. nov. A and B, skull and mandible in lateral views. C and D, close-up of external ear chamber in lateral and slightly ventral views; E and F, close-up of post-infratemporal fenestra on right side in lateral and slightly ventral views. Zigzag lines indicate a broken surface and fields of circles/dots indicate matrix. Abbreviations as listed in the text. **Page-size**

Figure 4. Photographs and corresponding line drawings of skull and mandible of *Eurycephalosuchus gannanensis* gen. and sp. nov. A and B, Skull and mandible in ventral views. C (derived from 3D image) and D, close-up of posteroventral part of skull and mandible in lateral and slightly dorsal views. Zigzag lines indicate a broken surface. Abbreviations as listed in the text. **Page-size**

Figure 5. Photographs and corresponding line drawings of skull and mandible of *Eurycephalosuchus gannanensis* gen. and sp. nov. A and C, skull and mandible in occipital views. B (derived from 3D image) and D, close-up of posterior end of skull and mandible in medial and slightly posterior views; E (derived from 3D image) and F, close-up of axis in posterolateral and slightly dorsal views. Zigzag lines indicate a broken surface and fields of circles/dots indicate the matrix. Abbreviations as listed in the text. **Page-size**

Figure 6. Photographs of dentition of *Eurycephalosuchus gannanensis* gen. and sp. nov. A, close-up of premaxillary dentition in anterior view; B, close-up of the 4th dentary tooth in lateral view; C, close-up of the first five maxillary teeth in lateral and slightly ventral view; D, close-up of the 6th and 7th maxillary teeth and the 12th dentary tooth in lateral view; E, close-up of the 7th to 9th maxillary teeth and the 12th dentary tooth in lateral view.; F, the 10th to 14th maxillary teeth in lateral view. Abbreviations as listed in the text. **Page-size**

Figure 7. Photographs (derived from 3D image) and corresponding line drawings of the 3rd cervical vertebra of *Eurycephalosuchus gannanensis* gen. and sp. nov. A and B, in anterolateral views; C and D, in posterior views; E and F, in lateral views; G and H, in

ventral views. Zigzag lines indicate a broken surface. Abbreviations as in the text. **Page-size**

Figure 8. Photographs (derived from 3D image) and corresponding line drawings of the 4th cervical (A to H) and the 12th (I and J) vertebrae of *Eurycephalosuchus gannanensis* gen. and sp. nov. A and E, in lateral views; B and F, in anterior views; C and G, in posterior views; D to J, in ventral views. Zigzag lines indicate a broken surface. Abbreviations as in the text. **Page-size**

Figure 9. Preserved postcranial section of *Eurycephalosuchus gannanensis* gen. and sp. nov. Photograph (A derived from 3D image) and corresponding line drawing (B) mainly in ventral view. Zigzag lines indicate a broken surface. Abbreviations as listed in the text. **Page-size**

Figure 10. Photographs of osteoderms of *Eurycephalosuchus gannanensis* gen. and sp. nov. A, preserved osteoderms with other postcranial elements; B to D, individual osteoderms in dorsal view; E, a ventral osteoderm in external view; F, an osteoderm from dorsolateral part of body in dorsal view. **Page-size**

Figure 11. Photographs and corresponding line drawings of scapulae and coracoids of *Eurycephalosuchus* gen. nov. A and E, scapula of *Eurycephalosuchus gannanensis* gen. and sp. nov. in lateral views; B and F, scapula and coracoid of *Eurycephalosuchus* sp. indet. in lateral views, C (derived from 3D image) and D, scapula and coracoid of *Eurycephalosuchus* sp. indet. in posterolateral and slightly ventral views; G (derived from 3D image), H and I (derived from 3D image), coracoid of *Eurycephalosuchus gannanensis* gen. and sp. nov. in external and internal views, respectively; J (derived from 3D image), scapula and coracoid of *Eurycephalosuchus* sp. indet. in external and

slightly posterior view. Zigzag lines indicate a broken surface. Abbreviations as in the text. **Page-size**

Figure 12. Photographs and corresponding line drawings of left humerus of *Eurycephalosuchus gannanensis* gen. and sp. nov. A and G, in anterior views; B and H, in lateral views; C and I, in medial views; D and J, in posterior views; E and K, distal/bottom views; F and L, proximal/top views. Zigzag lines indicate a broken surface. Abbreviations as in the text. **Page-size**

Figure 13. Strict consensus of the eight MPTs obtained by the analysis of the data matrix (124 taxa and 191 characters, with *Asiatosuchus nanlingensis* excluded). Bremer support values are listed at each node, showing a weak level of support for the clades of interests. **Page-size**

Table 1. Measurements of selected skull elements. Units = cm, † = preserved length or width, * = estimated length or width.

Elements	Measurements	Elements
Skull length (snout to quadrate condyles)	15.87†/16.37*	Length of 3rd vertebral centrum
Skull length (snout to posterior edge of skull table)	14.31†/14.81*	Length of 4th vertebral centrum
Skull width (across 5th maxillary teeth)	9.64	Length of 5th vertebral centrum
Skull width (across quadratojugals)	14.81	Length of 6th vertebral centrum
Length of snout (preorbital region)	9.635	Length of 7th vertebral centrum
Width of snout (across anterior margins of orbits	10.12	Length of 8th vertebral centrum
Length of postorbital region (to posterior edge of skull table--left)	5.37†/5.87*	Length of 9th vertebral centrum
Length of skull table (across centre of supratemporal fenestrae)	3.55	Length of 10th vertebral centrum
Width of skull table (across centre of supratemporal fenestrae)	8.55	Length of 11th vertebral centrum
Length of mandible (right ramus)	17.15	Length of 12th vertebral centrum
Length of mandible (left ramus)	18.3	Length of 13th vertebral centrum

Length of external naris	1.73	Length of 14th vertebral centrum
Width of external naris	2.86	Length of 15th vertebral centrum
Length of supratemporal fossa (left)	1.73†/2.0*	Length of interclavicle
Width of supratemporal fossa (left)	2.09	Length of humerus
Length of ventral margin of infratemporal fenestra (left)	2.15	Minimal width of humeral shaft
Length of incisive foramen	0.98	Length of small coracoid
Width of incisive foramen	1.56	Minimal width of small coracoid
Length of suborbital fenestra (left)	4.0†/4.5*	Minimal width of small scapula
Width of suborbital fenestra (left)	1.82	Length of big coracoid (IVPP V 31267)
Maximal height of external mandibular fenestra (left)	1.71	Minimal width of big coracoid (IVPP V 312
Maximal width of external mandibular fenestra (left)	1.18	Minimal width of big scapula (IVPP V 3126
Length of axis (with odontoid process)	2.51	Hight (length) of big scapula (IVPP V 31267

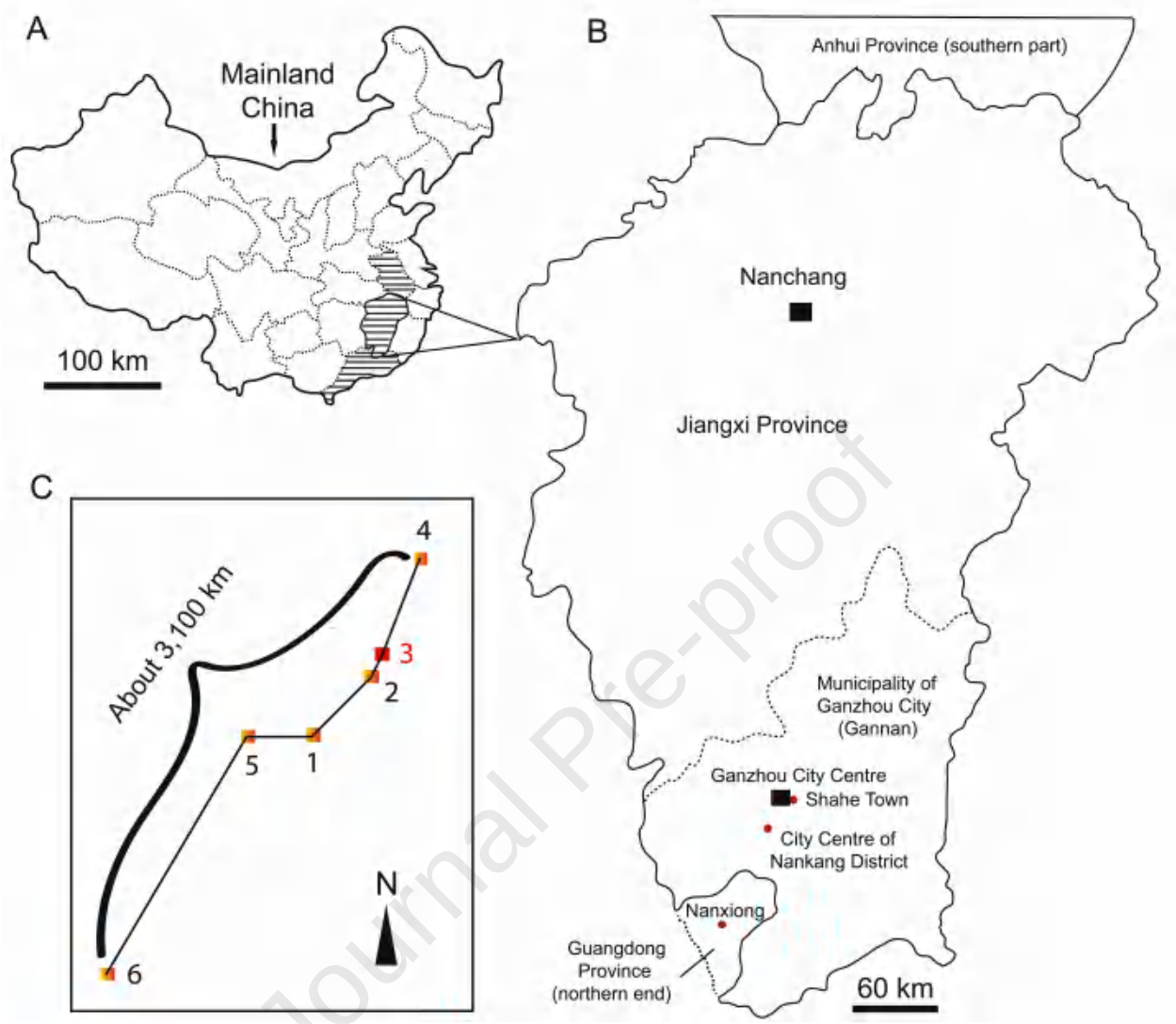

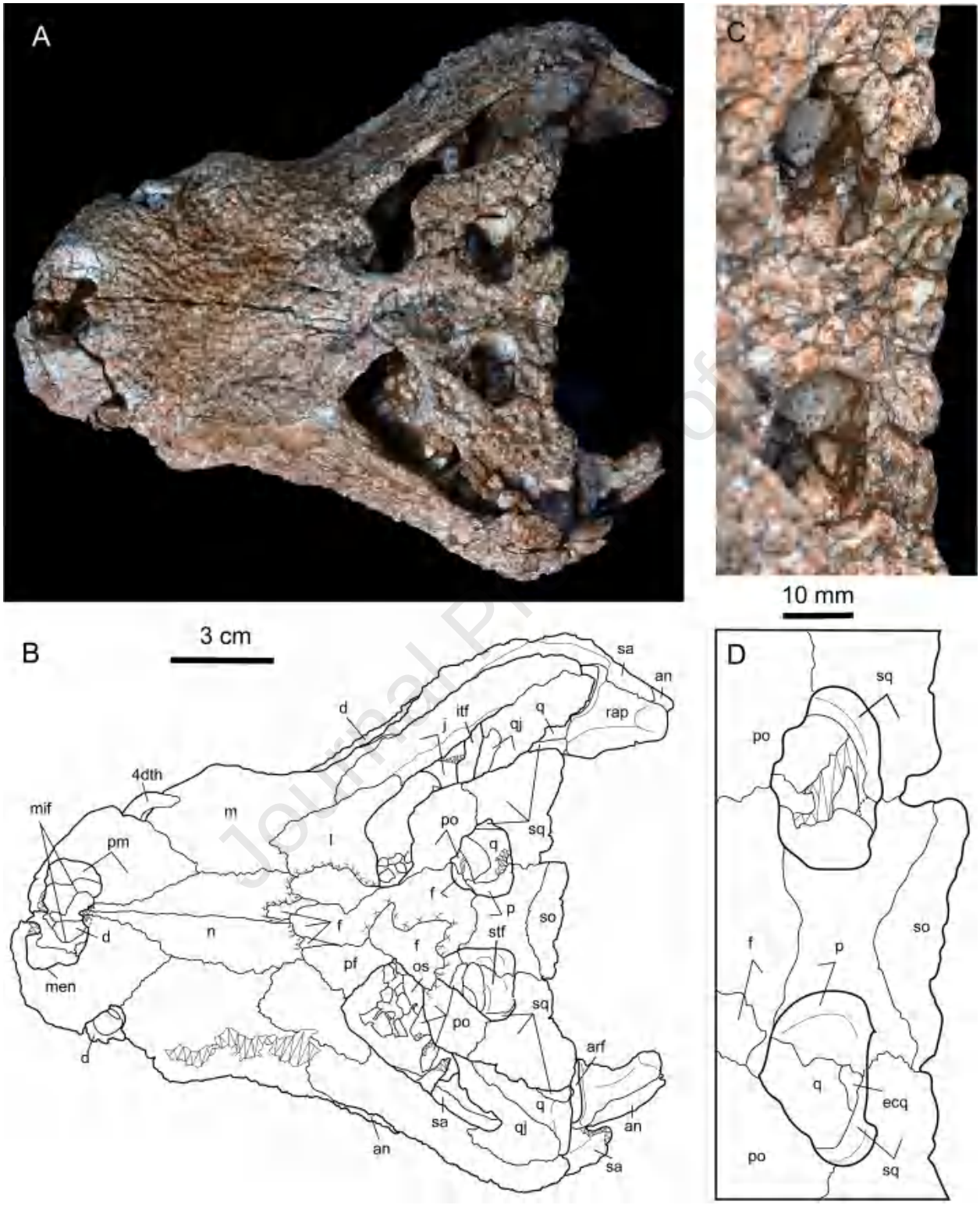
A
C
10 mm
B
3 cm
D
sa
an
rap
d
itf
j
qj
q
4dth
mif
m
pm
l
po
sq
f
p
so
n
stf
os
pf
men
arf
ecq
ect

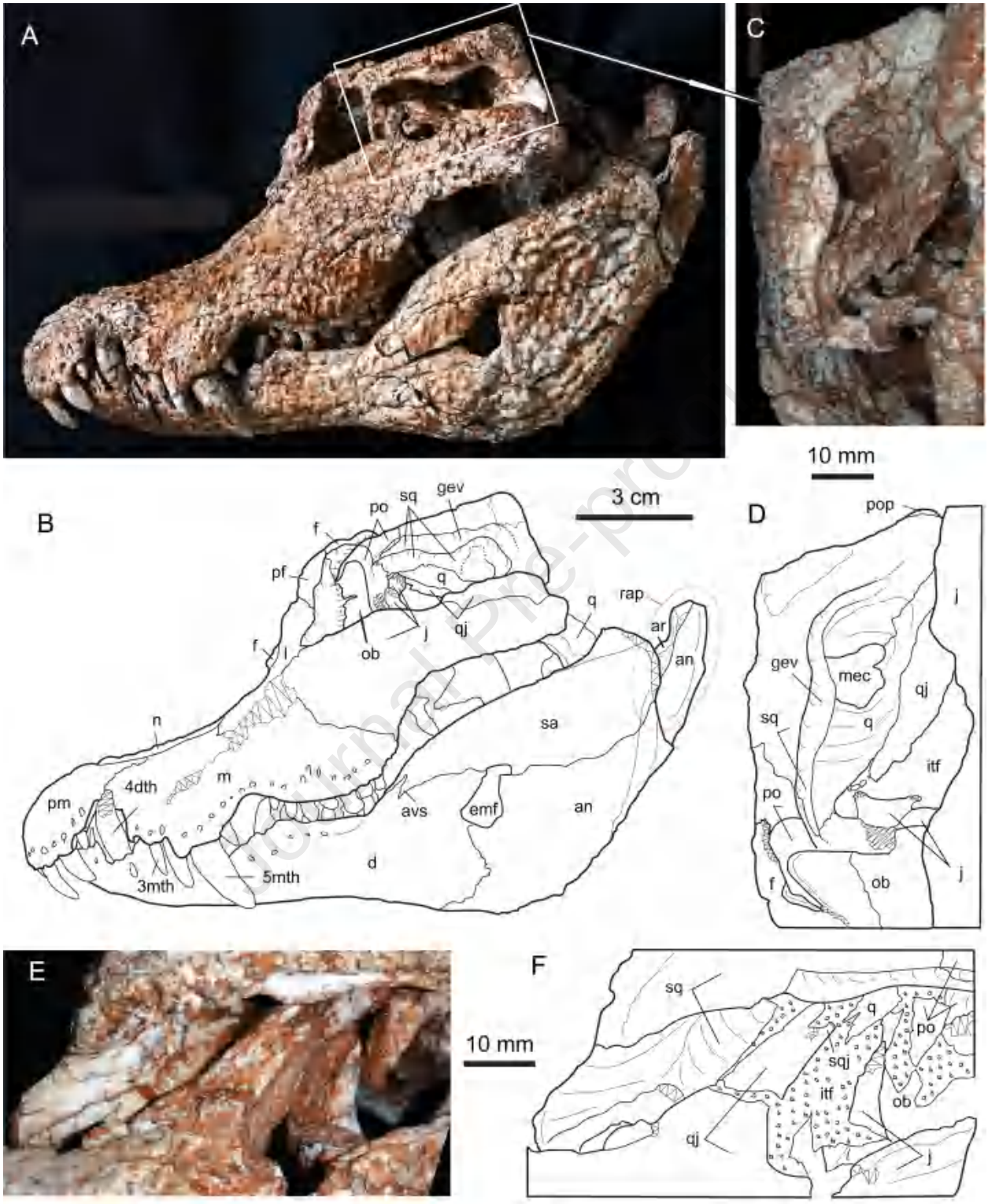
A
C
10 mm
B
3 cm
D
E
F
10 mm
sq
gev
po
f
pf
q
rap
ar
an
qj
j
ob
l
n
sa
m
4dth
pm
avs
emf
an
d
3mth
5mth
pop
mec
itf
sqj

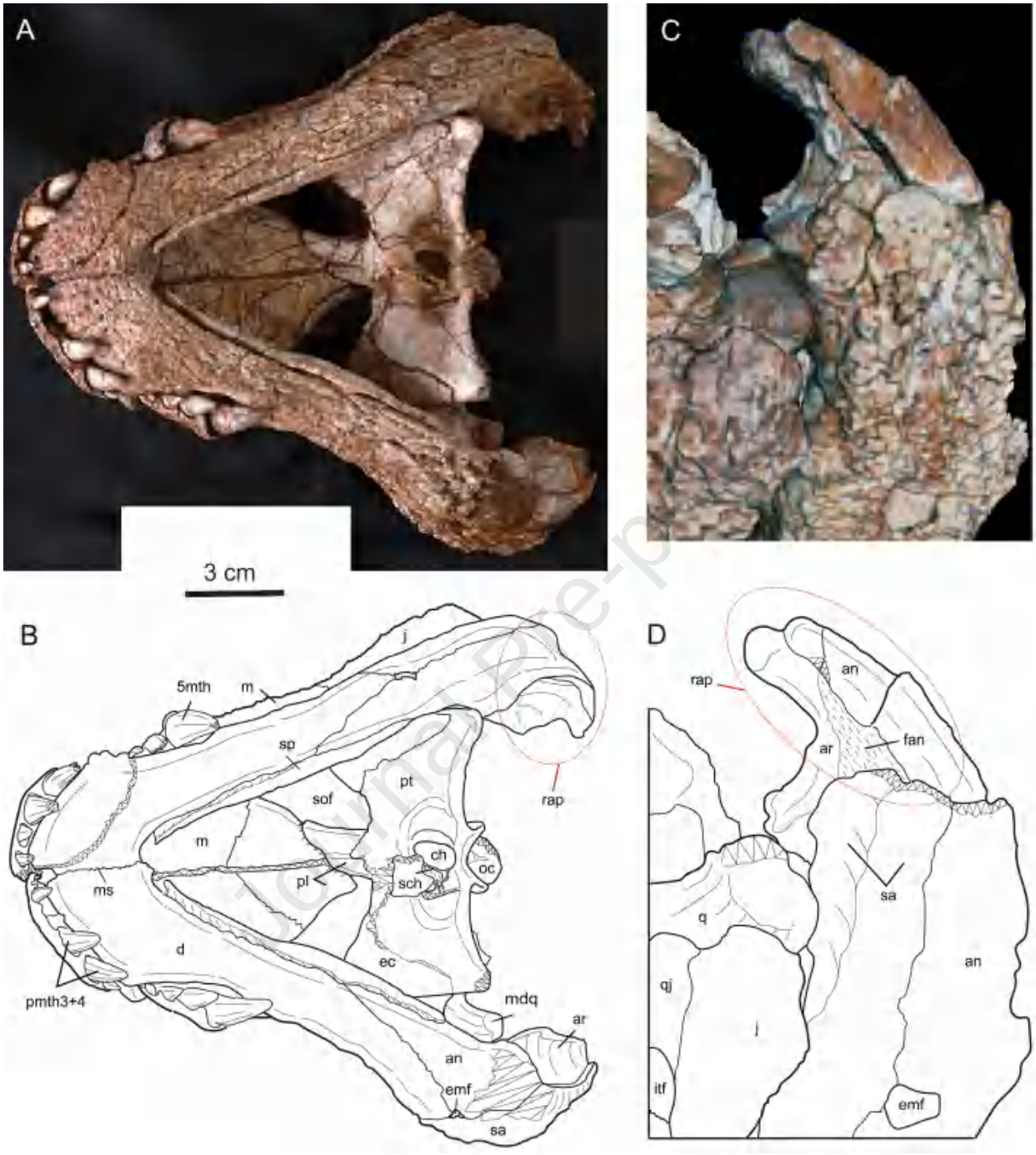
A
3 cm
C
B
5mth
m
j
sp
sof
pt
rap
m
ch
oc
ms
pl
sch
d
ec
pmth3+4
mdq
ar
an
emf
sa
D
rap
an
ar
fan
sa
q
an
qj
j
itf
emf

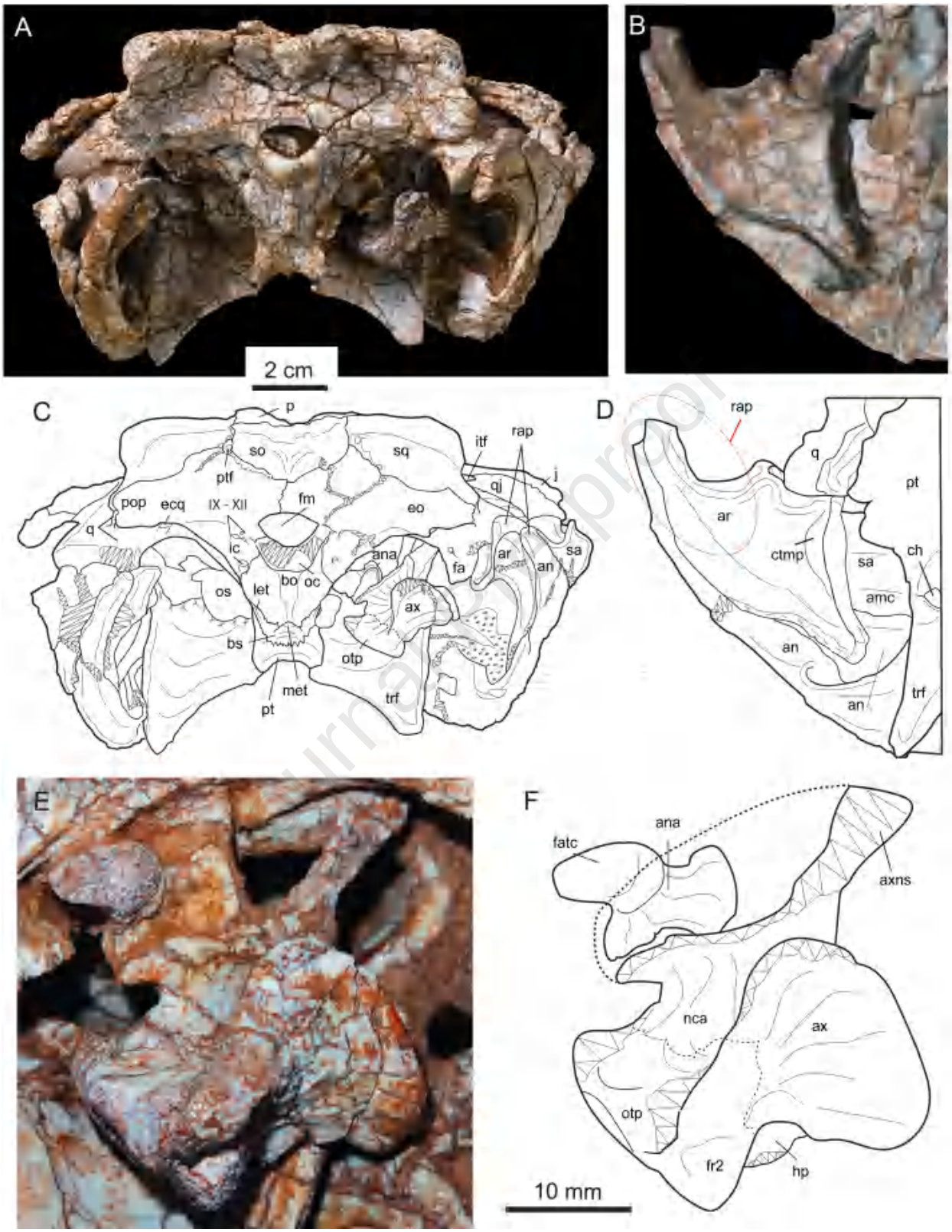
A
B
2 cm
C
p
so
sq
itf
rap
ptf
qj
j
pop
ecq
IX - XII
fm
eo
q
ic
ana
fa
ar
an
sa
os
let
bo
oc
ax
bs
otp
met
pt
trf
D
rap
q
pt
ar
ctmp
sa
ch
amc
an
an
trf
E
F
ana
fatc
axns
nca
ax
otp
fr2
hp
10 mm

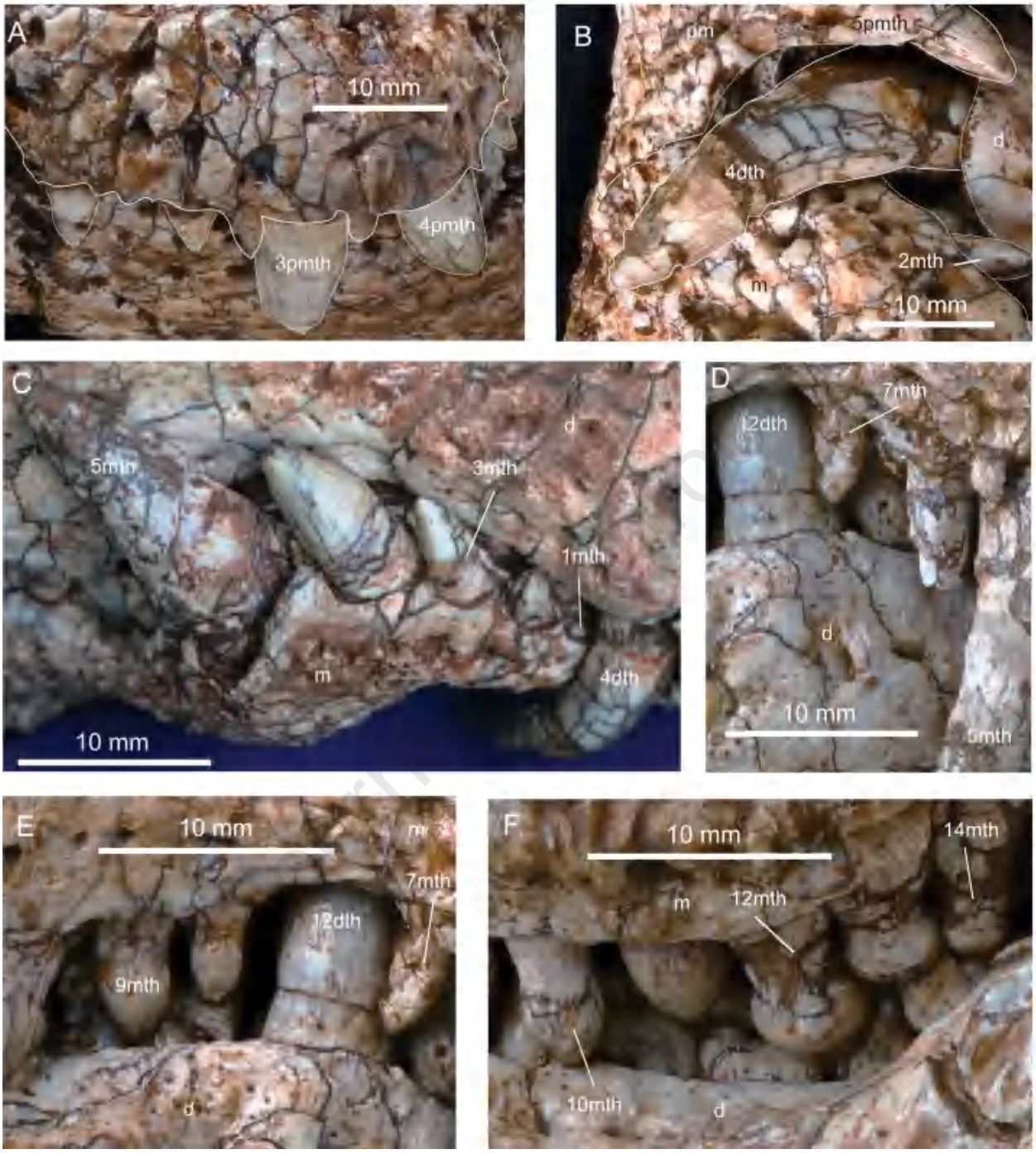
A
10 mm
4pmth
3pmth
B
pm
5pmth
d
4dth
2mth
m
10 mm
C
d
5mth
3mth
1mth
m
4dth
10 mm
D
7mth
12dth
d
10 mm
E
10 mm
m
7mth
12dth
9mth
d
F
10 mm
14mth
m
12mth
10mth
d

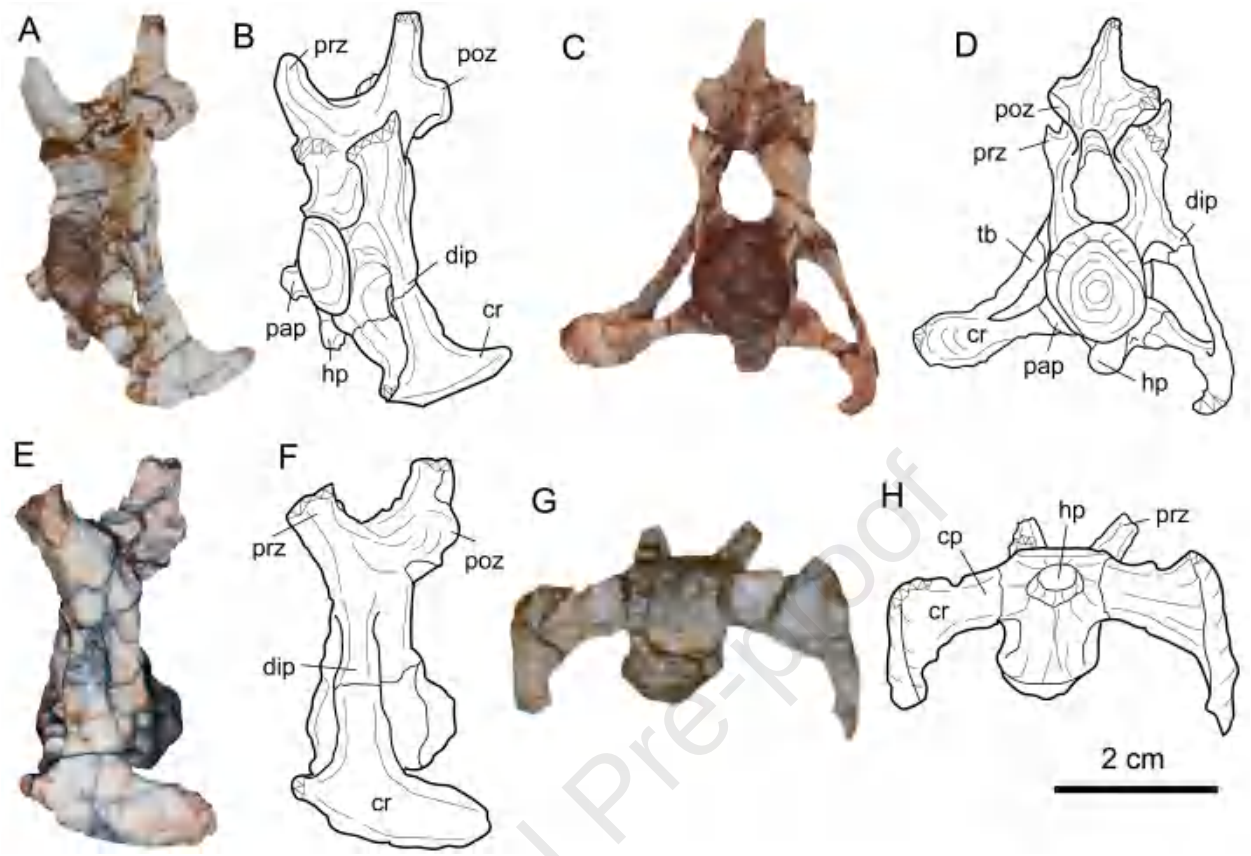

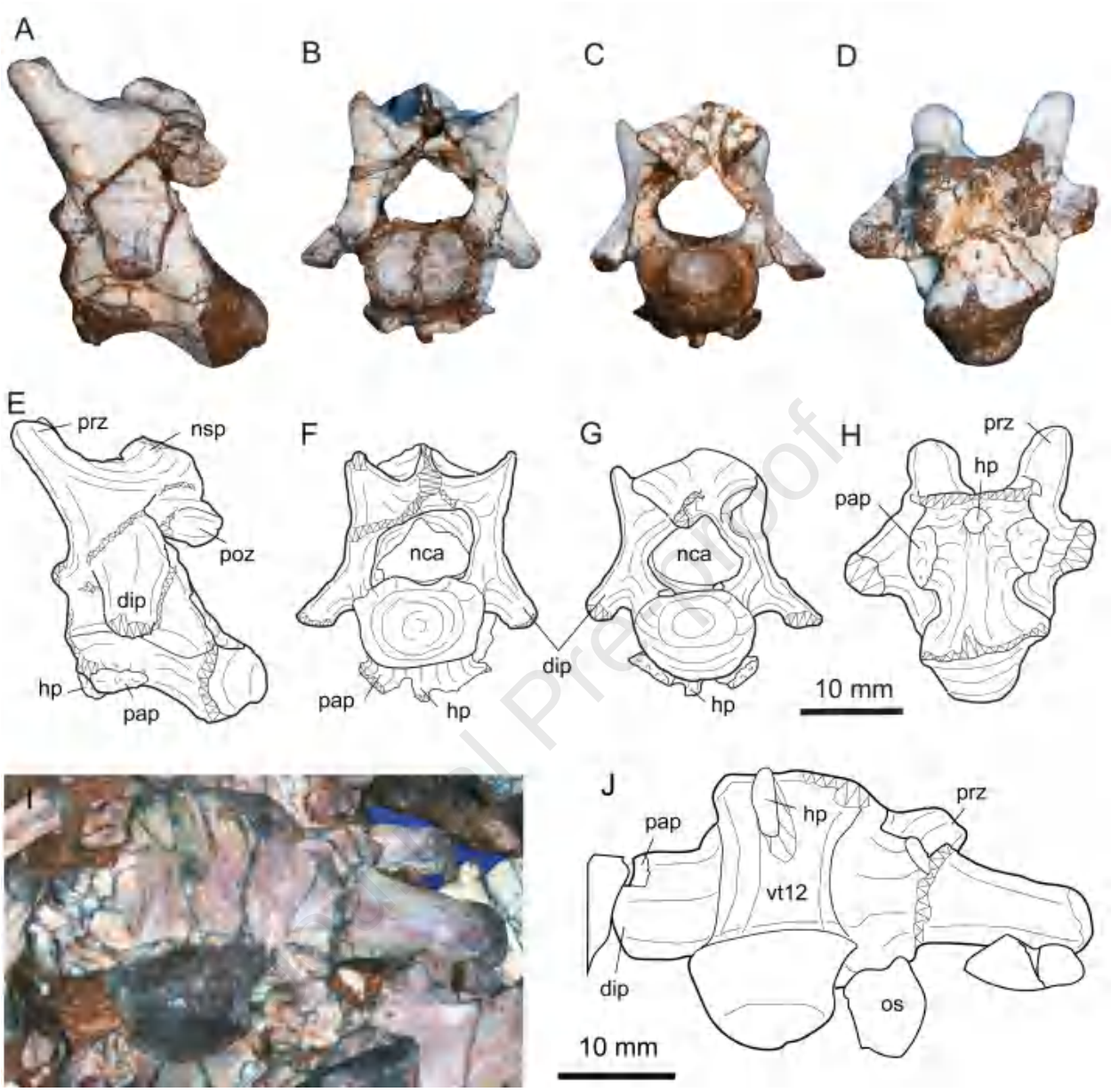

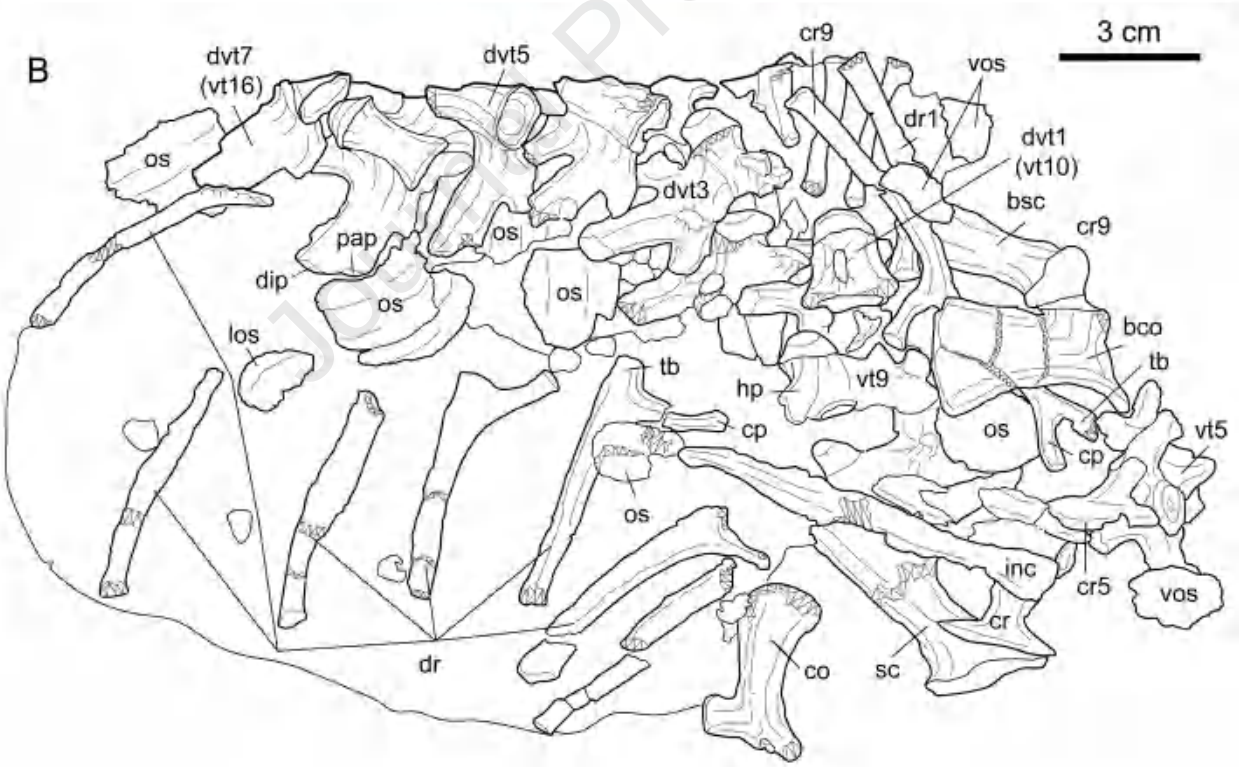
B
3 cm
dvt7
(vt16)
dvt5
cr9
vos
dr1
dvt1
(vt10)
os
dvt3
bsc
cr9
pap
os
dip
os
os
bco
los
tb
tb
hp
vt9
cp
os
cp
vt5
os
inc
cr5
vos
cr
dr
co
sc

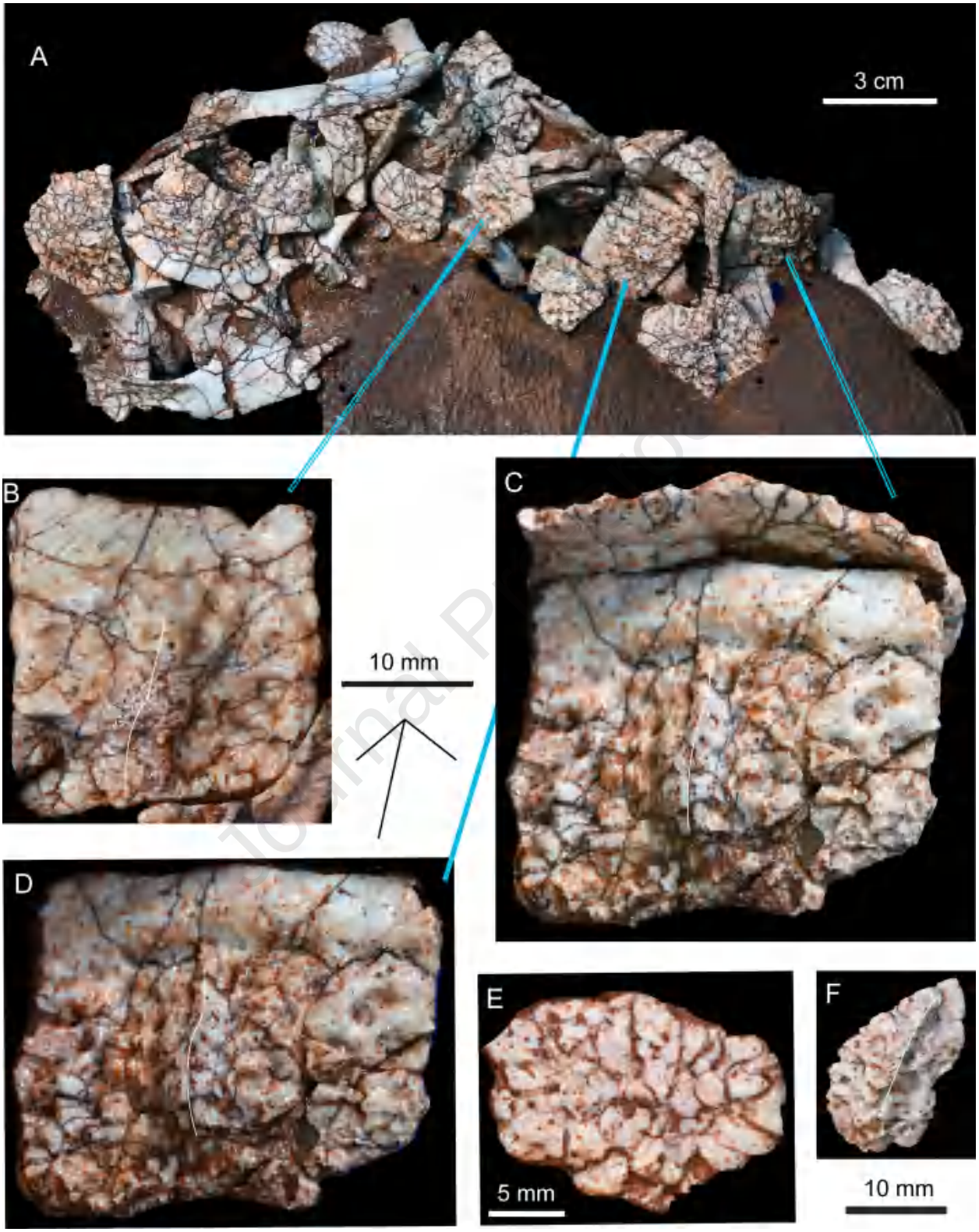
A
3 cm
B
10 mm
C
D
E
5 mm
F
10 mm

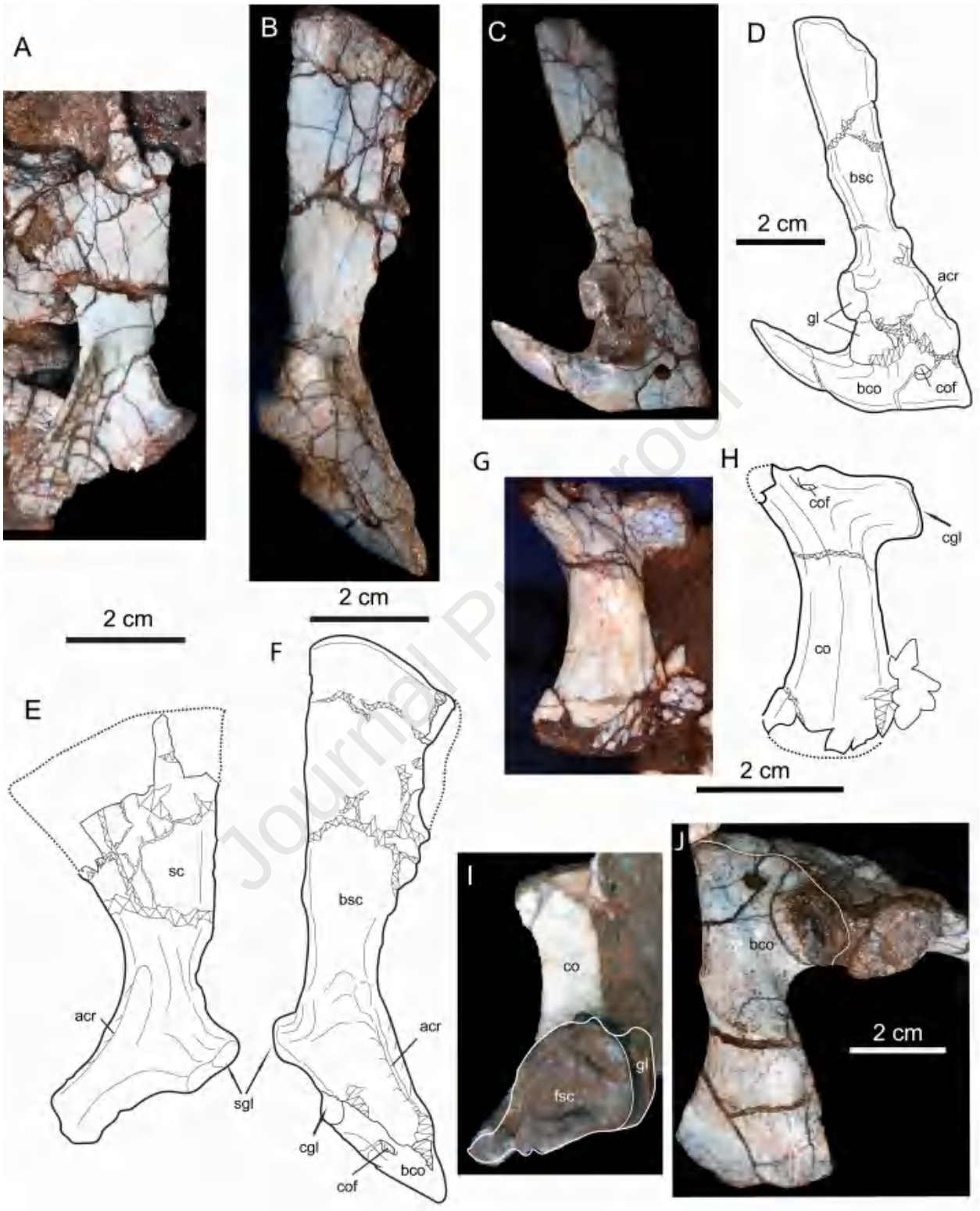

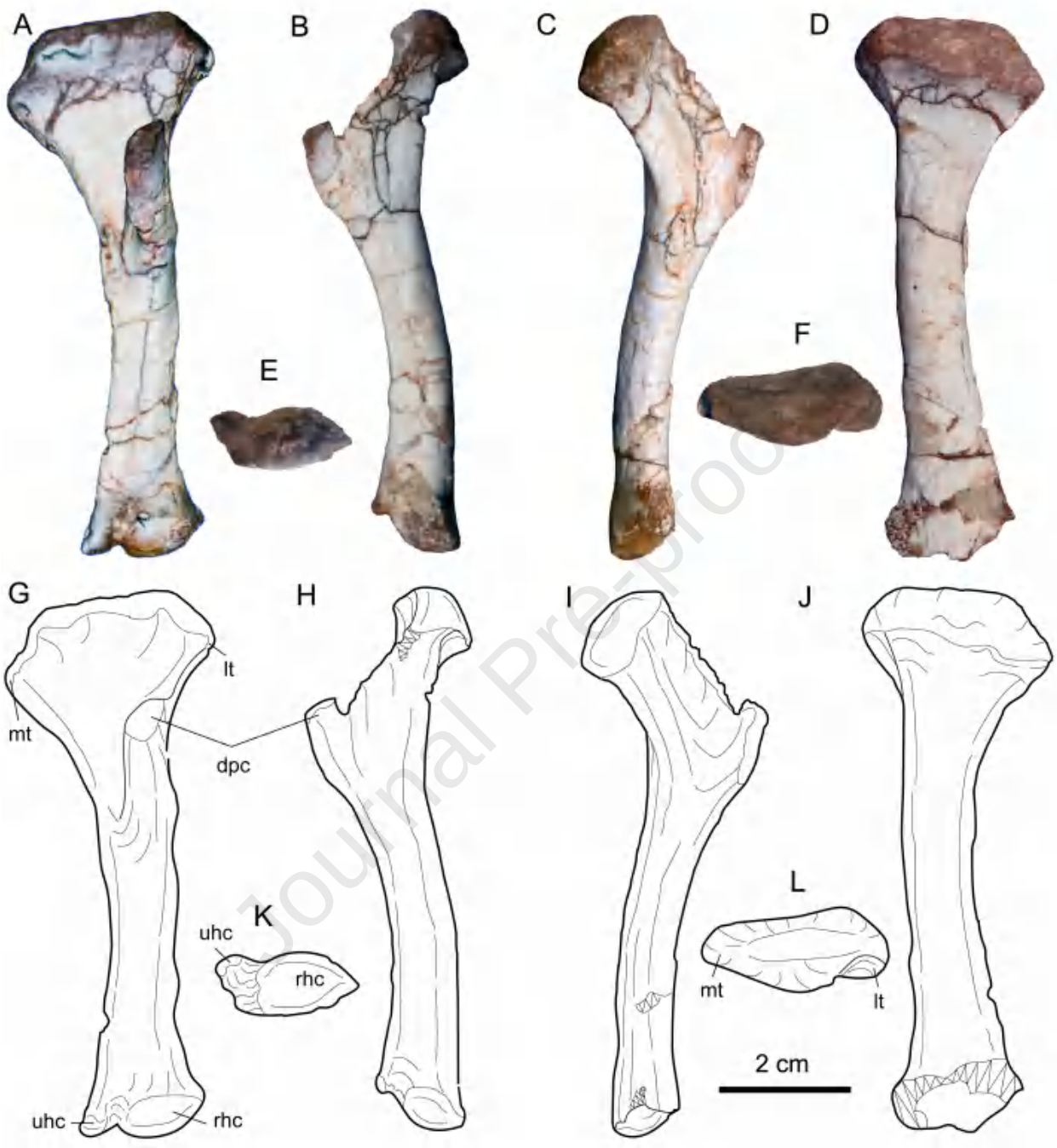

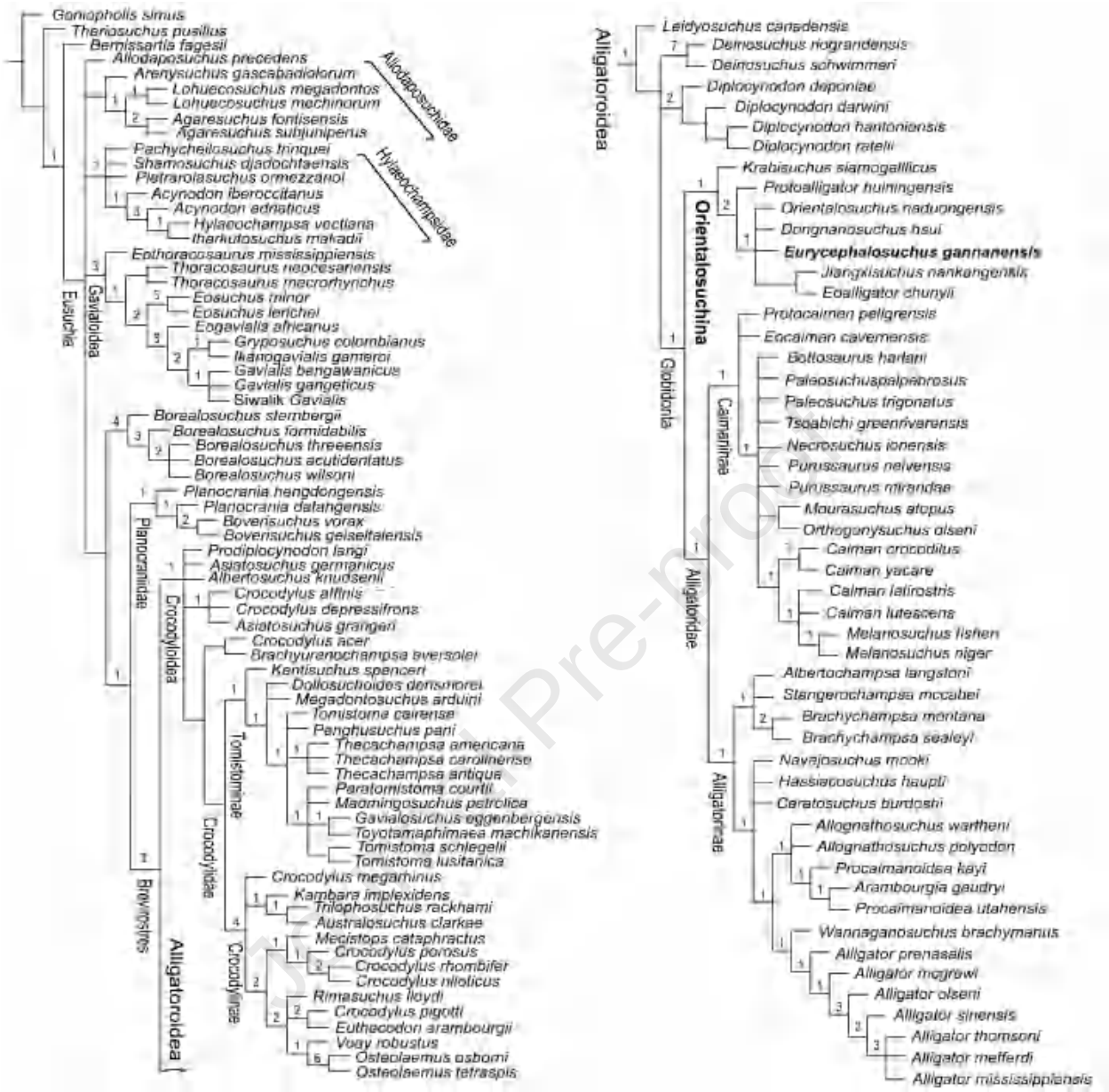
Goniopholis simus
Theriosuchus pusillus
Bernissartia fagesii
Allodaposuchus precedens
Arenysuchus gascabadiolorum
Lohuecosuchus megadontos
Lohuecosuchus mechinorum
Agaresuchus fontisensis
Agaresuchus subjuniperus
Pachycheilosuchus trinquei
Shamosuchus djadochtaensis
Pietraroiasuchus ormezzanoi
Acynodon iberoccitanus
Acynodon adriaticus
Hylaeochampsa vectiana
Iharkutosuchus makadi
Allodaposuchidae
Hylaeochampsidae
Eusuchia
Gavialoidea
Epthoracosaurus mississippiensis
Thoracosaurus neocesariensis
Thoracosaurus macrorhynchus
Eosuchus minor
Eosuchus lerichei
Eogavialis africanus
Gryposuchus colombianus
Ikanogavialis gameroi
Gavialis bengawanicus
Gavialis gangeticus
Siwalik Gavialis
Borealosuchus sternbergi
Borealosuchus formidabilis
Borealosuchus threeensis
Borealosuchus acutidentatus
Borealosuchus wilsoni
Planocrania hengdongensis
Planocrania datangensis
Boverisuchus vorax
Boverisuchus geiseltalensis
Prodiplocynodon langi
Asiatosuchus germanicus
Albertosuchus knudseni
Planocraniidae
Crocodylia
Crocodyloidea
Crocodylus affinis
Crocodylus depressifrons
Asiatosuchus grangeri
Crocodylus acer
Brachyuranochampsa eversoler
Kentisuchus spenceri
Dollosuchoides densmorei
Megadontosuchus arduini
Tomistoma cairense
Panghusuchus pani
Thecachampsa americana
Thecachampsa carolinense
Thecachampsa antiqua
Paratomistoma courtii
Maomingosuchus petrolica
Gavialosuchus eggenbergensis
Toyotamaphimaea machikanensis
Tomistoma schlegelii
Tomistoma lusitanica
Tomistominae
Crocodylidae
Crocodylus megarhinus
Kambara implexidens
Trilophosuchus rackhami
Australosuchus clarkae
Mecistops cataphractus
Crocodylus porosus
Crocodylus rhombifer
Crocodylus niloticus
Rimasuchus lloydi
Crocodylus pigotti
Euthecodon arambourgii
Voay robustus
Osteolaemus osborni
Osteolaemus tetraspis
Crocodylinae
Brevirostres
Alligatoroidea
Alligatoroidea
Leidyosuchus canadensis
Deinosuchus riograndensis
Deinosuchus schwimmeri
Diplocynodon deponiae
Diplocynodon darwini
Diplocynodon hantoniensis
Diplocynodon ratelii
Krabisuchus siamogallicus
Protoalligator huiningensis
Orientalosuchus naduongensis
Dongnanosuchus hsui
Eurycephalosuchus gannanensis
Jiangxisuchus nankangensis
Eoalligator chunyii
Orientalosuchina
Globidonta
Protocaiman peligrensis
Eocaiman cavernensis
Bottosaurus harlani
Paleosuchus palpebrosus
Paleosuchus trigonatus
Tsoabichi greenriverensis
Necrosuchus ionensis
Purussaurus neivensis
Purussaurus mirandae
Mourasuchus atopus
Orthogenysuchus olseni
Caiman crocodilus
Caiman yacare
Caiman latirostris
Caiman lutescens
Melanosuchus fisheri
Melanosuchus niger
Caimaninae
Alligatoridae
Albertochampsa langstoni
Stangerochampsa mccabei
Brachychampsa montana
Brachychampsa sealeyi
Navajosuchus mooki
Hassiacosuchus haupti
Ceratosuchus burdoshi
Allognathosuchus warthen
Allognathosuchus polyodon
Procaimanoidea kayi
Arambourgia gaudryi
Procaimanoidea utahensis
Wannaganosuchus brachymanus
Alligator prenasalis
Alligator mcgrewi
Alligator olseni
Alligator sinensis
Alligator thomsoni
Alligator mefferdi
Alligator mississippiensis
Alligatorinae

Declaration of interests

☒ The authors declare that they have no known competing financial interests or personal relationships that could have appeared to influence the work reported in this paper.

☐The authors declare the following financial interests/personal relationships which may be considered as potential competing interests: